

AD-A114 672

HONEYWELL POWER SOURCES CENTER HORSHAM PA  
HIGH EFFICIENCY LITHIUM-THIONYL CHLORIDE CELL.(U)  
APR 82 N DODDAPANENI

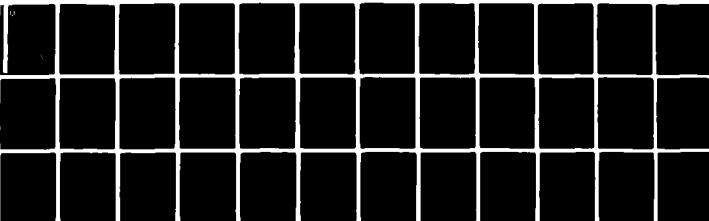
F/G 10/3

DAAK20-81-C-0381

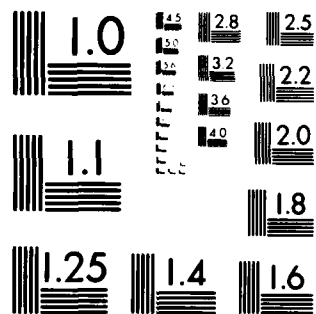
UNCLASSIFIED

DELET-TR-81-0381-3

NL



END  
DATE  
FILMED  
6 42  
DTIC



MICROCOPY RESOLUTION TEST CHART  
NATIONAL BUREAU OF STANDARDS 1963-A



Research and Development Technical Report

■

DELET-TR-81-0381-3

HIGH EFFICIENCY LITHIUM-THIONYL CHLORIDE CELL

Dr. N. Doddapaneni  
Honeywell Power Sources Center  
104 Rock Road  
Horsham, PA 19044

April 1982

THIRD QUARTERLY for PERIOD 9 OCTOBER 1981 - 8 JANUARY 1982

APPROVED FOR PUBLIC RELEASE: DISTRIBUTION UNLIMITED

Prepared for:

ELECTRONICS TECHNOLOGY AND DEVICES LABORATORY

DCASMA, PHILADELPHIA  
P. O. BOX 7699  
PHILADELPHIA, PA 19101

DTIC  
ELECTE  
S MAY 20 1982 D  
A

DTIC FILE COPY

ERADCOM

US ARMY ELECTRONICS RESEARCH AND DEVELOPMENT COMMAND  
FORT MONMOUTH, NEW JERSEY 07703

82 05 19 050

HISA-FM 195-78

AD A114672

## **NOTICES**

### **Disclaimers**

The citation of trade names and names of manufacturers in this report is not to be construed as official Government indorsement or approval of commercial products or services referenced herein.

### **Disposition**

Destroy this report when it is no longer needed. Do not return it to the originator.

Unclassified

REPORT DOCUMENTATION PAGE		READ INSTRUCTIONS BEFORE COMPLETING FORM
1. REPORT NUMBER DELET-TR-81-0381-3	2. GOVT ACCESSION NO.	3. RECIPIENT'S CATALOG NUMBER
4. TITLE (and Subtitle)  High Efficiency Lithium-Thionyl Chloride Cell		5. TYPE OF REPORT & PERIOD COVERED 10-9-81 to 1-8-82 Third Quarterly
		6. PERFORMING ORG. REPORT NUMBER
7. AUTHOR(s)  N. Doddapaneni		8. CONTRACT OR GRANT NUMBER(s)  DAAK20-81-C-0381
9. PERFORMING ORGANIZATION NAME AND ADDRESS Honeywell Power Sources Center 104 Rock Road Horsham, Pa. 19044		10. PROGRAM ELEMENT, PROJECT, TASK AREA & WORK UNIT NUMBERS  1L162705AH94-11-211
11. CONTROLLING OFFICE NAME AND ADDRESS U.S. Army Elct Tech & Dvcs Laboratory ATTN: DELET-PR Fort Monmouth, NJ 07703		12. REPORT DATE April 1982
14. MONITORING AGENCY NAME & ADDRESS (if different from Controlling Office) DCASMA, Philadelphia P.O. Box 7699 Philadelphia, Pa. 19101		13. NUMBER OF PAGES 37 pages
		15. SECURITY CLASS. (of this report) Unclassified
15a. DECLASSIFICATION/DOWNGRADING SCHEDULE		
16. DISTRIBUTION STATEMENT (of this Report)  Approved for Public Release: Distribution Unlimited		
17. DISTRIBUTION STATEMENT (of the abstract entered in Block 20, if different from Report)		
18. SUPPLEMENTARY NOTES		
19. KEY WORDS (Continue on reverse side if necessary and identify by block number) Thionyl chloride, lithium, high discharge rates, low temperatures, catalysis, cyclic voltammetry		
20. ABSTRACT (Continue on reverse side if necessary and identify by block number)  During the third quarter, cathode optimization with respect to specified variables was completed. Performance evaluation of optimized cathodes at 32° and 75° F showed both catalyst B and C (FePc) and (CoPc) <sub>(n)</sub> minimized the electrode overpotential.  Plots of <del>1-1</del> vs <del>ω</del> <sup>-1/2</sup> from rotating disc electrode studies produced		

Unclassified

parallel straight lines, indicative of a first order reaction mechanism. The slope of the straight line decreased with FePc catalyzed cathodes. This could indicate a change in reaction mechanism.

AC impedance measurements of a carbon electrode indicated extremely slow charge transfer and at high discharge rates, the rates were purely diffusion controlled.

Unclassified

SECURITY CLASSIFICATION OF THIS PAGE(When Data Entered)

# TABLE OF CONTENTS

	<u>Page</u>
I INTRODUCTION	1
II EVALUATION OF CATHODE OVERPOTENTIAL	3
III KINETIC AND MECHANISTIC STUDIES	19
IV AC IMPEDANCE MEASUREMENTS	24
V SUMMARY AND FUTURE WORK	33
DISTRIBUTION	35



Accession For	
DTIC GRA&I	<input checked="" type="checkbox"/>
DTIC TAB	<input type="checkbox"/>
Unannounced	<input type="checkbox"/>
Justification	
By	
Distribution/	
Availability Codes	
Dist. Statement	
Dist. Statement	

# LIST OF FIGURES

	<u>Page</u>
1. Effect of Cathode Variables on Li/SOCl <sub>2</sub> Cell Life with 50% SAB in 1.5M LiAlCl <sub>4</sub> /SOCl <sub>2</sub> at -20°F	4
2. Same, except 100% SAB	5
3. Same, except 5% (CoPc) <sub>n</sub>	6
4. Effect of Carbon Substrates on the Li/SOCl <sub>2</sub> Cell Discharge Time in 1.5M LiAlCl <sub>4</sub> /SOCl <sub>2</sub> at -20°F	7
5. Effect of Cathode Thickness on Discharge Characteristics of Li/SOCl <sub>2</sub> Cell, etc.	9
6. Effect of Cathode Thickness on Discharge Performance Characteristics	10
7. Effect of Cathode Thickness on Discharge Performance, etc.	11
8. Effect of Cathode Thickness on Discharge Characteristics, etc.	12
9. Polarization Characteristics at 75°F	14
10. Discharge Characteristics at 10 mA/cm <sup>2</sup> and 75°F	15
11. " " " 20 mA/cm <sup>2</sup> " "	16
12. " " " 10 mA/cm <sup>2</sup> and 32°F	17
13. " " " 20 mA/cm <sup>2</sup> and 32°F	18
14. Plot of 1/i <sub>p</sub> VS 1/√ω From the Rotating Disc Data	21
15. " " " " " " " "	22
16. " " " " " " " "	23
17. Impedance of Stress Annealed Pyrolytic Graphite Electrode	27
18. " " " " " "	28
19. " " " " " "	29
20. " " " " " "	30
21. " " " " " "	31
22. " " " " " "	32



## I. INTRODUCTION

The  $\text{Li/SOCl}_2$  system<sup>(1-4)</sup> has the potential to be one of the best primary batteries having combined characteristics of high rate and high energy density capability, long shelf-life and wide operating temperature range. However, many of these advantages have not been fully derived. The operating capabilities of  $\text{Li/SOCl}_2$  batteries are limited, to a large extent, by the Teflon bonded porous carbon electrode commonly used as a cathode. Cell failure at high discharge rates and/or low operating temperatures has, as one of its main causes, the high cathodic overpotential resulting from non-uniform current distribution over the porous electrode.

The porous carbon cathode, where the reduction of  $\text{SOCl}_2$  occurs, has a limited capacity for retaining solid lithium chloride as it precipitates in the pore structure. As the lithium chloride accumulates, the porosity of the electrode is reduced to where mass transport, particularly of the cathode depolarizer, can no longer be maintained at a rate sufficient to support the required current density. When this happens, polarization becomes excessive and denotes the end of useful battery life.

At high rate discharges and low operating temperatures, the cathode polarization problem becomes very severe. Analysis of the porous electrode shows that, at high rate discharges, only a small part of the available surface participates in the electrochemical process.

Cathode polarization and the reaction zone thickness strongly depend on electrode reactions, cathode thickness and composition. Minimization of the effects of these variables on overpotential is essential in order for  $\text{Li/SOCl}_2$  batteries to be viable electrochemical devices for many of the high rate/low temperature applications.

The objectives of this program, therefore, are to:

- Evaluate the polarization characteristics of Teflon-bonded porous carbon cathodes.
- Improve cathode performance at high discharge rates and low operating temperatures.

Polarization characteristics will be determined as a function of cathode thickness, composition and density, applied current density and temperature ( $-40^{\circ}\text{F}$  to  $75^{\circ}\text{F}$ ). Several experimental techniques such as half-cell measurements, discharge performance characteristics, impedance measurements, and cyclic voltammetry studies will be employed to evaluate the extent of each variable's contribution to the cathode polarization.

Improvement in cathode performance will be made by the use of electrocatalysis. Three catalysts employed in this program<sup>(5)</sup> have shown marked improvements in both cell voltage and cathode capacity. They were \*,

Catalyst A = Cobalt Phthalocyanine Monomer, CoPc

Catalyst B = Iron Phthalocyanine Monomer, FePc

Catalyst C = Polymeric Cobalt Phthalocyanine, (CoPc)<sub>n</sub>

During the first quarter of this program<sup>(6)</sup>, we examined:

- a) The overpotential of cathodes with and without Catalyst B and C, over a temperature range of  $-40$  to  $75^{\circ}\text{F}$ ,
- b) The effects of catalysts and temperatures on cyclic voltammograms in  $\text{LiAlCl}_4/\text{SOCl}_2$  electrolyte solutions.
- c) The effects of operating temperatures ( $-40$  to  $75^{\circ}\text{F}$ ) on the conductivity and viscosity of the electrolyte solutions ( $\text{LiAlCl}_4/\text{SOCl}_2$ ).

During the second quarter<sup>(7)</sup>, we completed the overpotential measurements at  $-20$  and  $-40^{\circ}\text{F}$  on our present baseline cathodes with and without catalysts. These cathodes contained 5% Teflon binder and had a thickness of 0.020 inch. Furthermore, we systematically evaluated the effect of cathode thickness, amount of Teflon binder, and cathode substrates on cathode performance.

During this reporting period, we examined:

- a) Polarization with respect to cathode variables.
- b) Performance of optimized cathodes.
- c) Cyclic voltammograms at rotating disc electrodes.
- d) AC impedance measurements of porous electrodes.

---

\* Patents pending

## II. EVALUATION OF CATHODE OVERPOTENTIAL

### A. CATHODE PERFORMANCE IMPROVEMENTS

#### 1. Introduction

The effect of carbon substrate, density and thickness of porous carbon cathodes on the overall performance of Li/SOCl<sub>2</sub> cells at 0°F and 75°F was reported in the second quarterly report<sup>(7)</sup>. During this period, the effect of cathode variables at -20 and -40°F were evaluated using catalyst C (CoPc)<sub>n</sub>. At these temperatures, the FePc catalyst was found to contribute severe voltage delay. Nevertheless, significant improvement in overall performance of Li/SOCl<sub>2</sub> cells was still achieved with this catalyst throughout the operating temperatures and discharge current rates studied.

#### 2. Electrochemical Cell Performance

Laboratory cells were built and tested with cathodes having several variables. Low temperature tests (-20 and -40°F) were conducted after allowing the cells to stand at operating temperature for 30-60 minutes. Even with the use of distilled thionyl chloride solvent (Mobay Chemicals), severe voltage delays at discharge rates of 5 or 10 mA/cm<sup>2</sup> were observed. To overcome this problem and thus allow catalyst C to be evaluated for rate improvement, the cells were subjected to a small discharge current (0.1 mA/cm<sup>2</sup>) during their stand time period.

Figures 1 through 3 show the effect of cathode thickness and density (as varied by composition) on discharge time. Both of these cathode variables affected cell life. The influence on discharge time by the cathode variables studied are compared in Figure 4. Even though discharge time increased with cathode thickness, the increase was not proportional to the thickness. Therefore, it should be noted that the reaction zone thickness depends strongly on cathode thickness, discharge rate and operating temperature. The lithium chloride deposition in the carbon pores might be creating the resistive film that is responsible for cathode polarization and hence cell life.

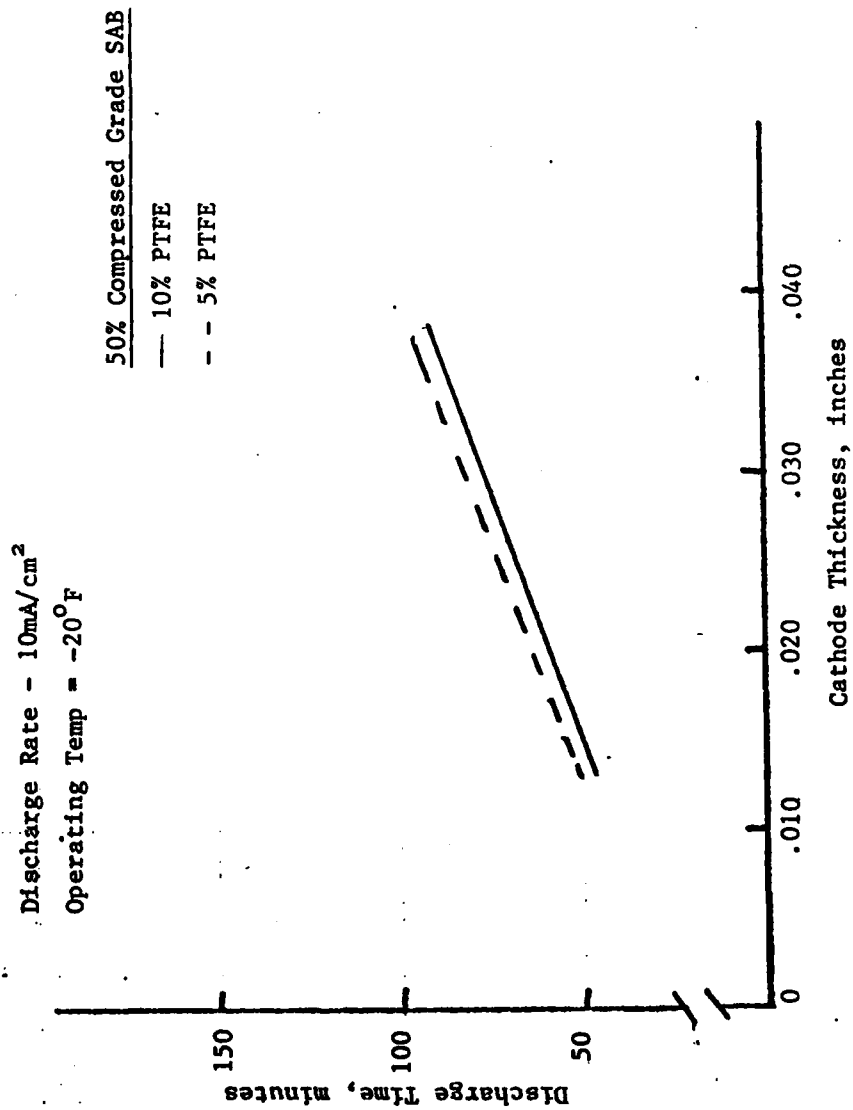


Figure 1. Effect of Cathode Variables on Li/SOCl<sub>2</sub> Cell Life with 50% SAB in 1.5M LiAlCl<sub>4</sub>/SOCl<sub>2</sub> at -20°F.

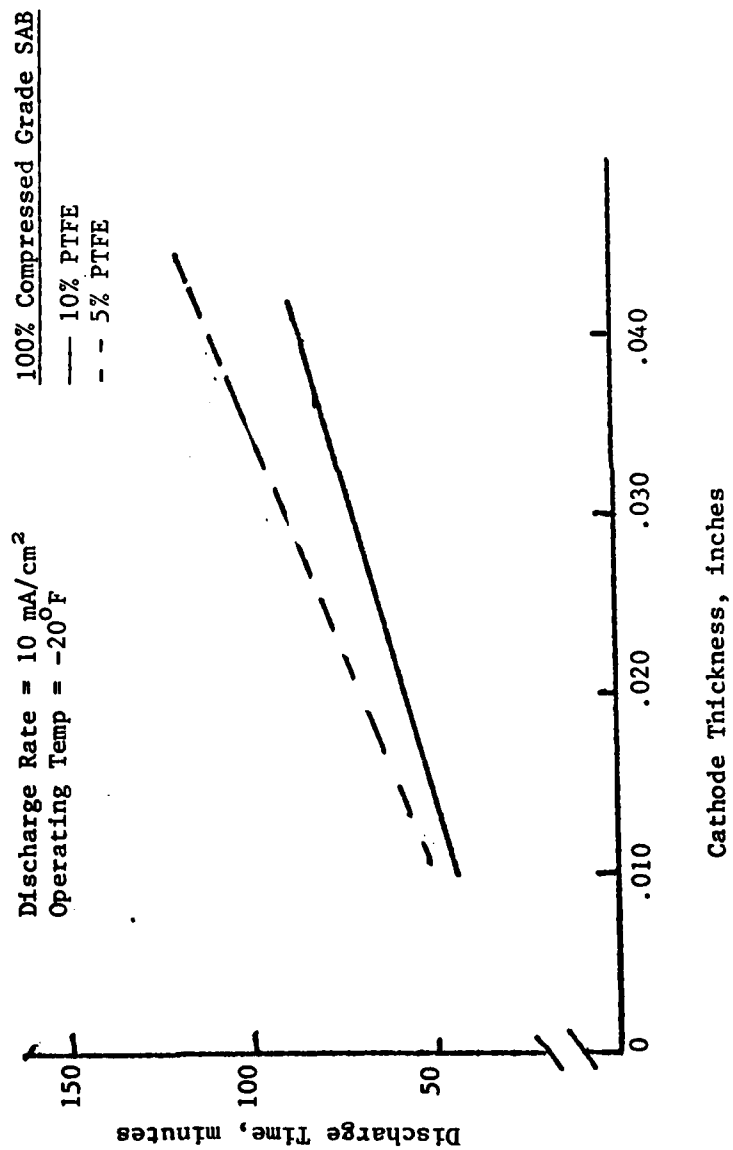


Figure 2. Effect of Cathode Variables on Li/SOCl<sub>2</sub> Cell Life with 100% SAB in 1.5M LiAlCl<sub>4</sub>/SOCl<sub>2</sub> at -20°F

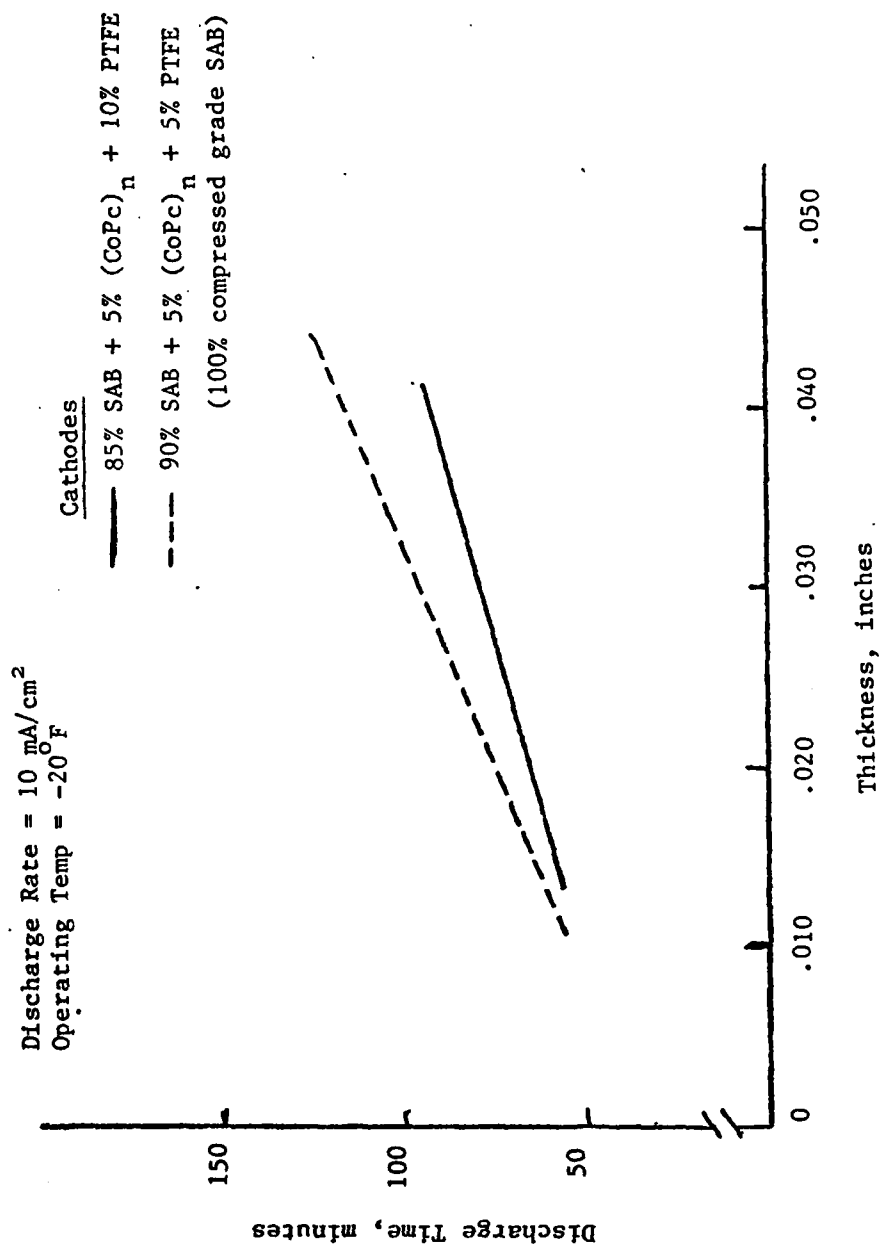


Figure 3. Effect of Cathode Variables on Li/SOCl<sub>2</sub> Cell Life with 5% (CoPc)<sub>n</sub>  
Catalyzed Cathodes in 1.5M LiAlCl<sub>4</sub>/SOCl<sub>2</sub> at -20°F

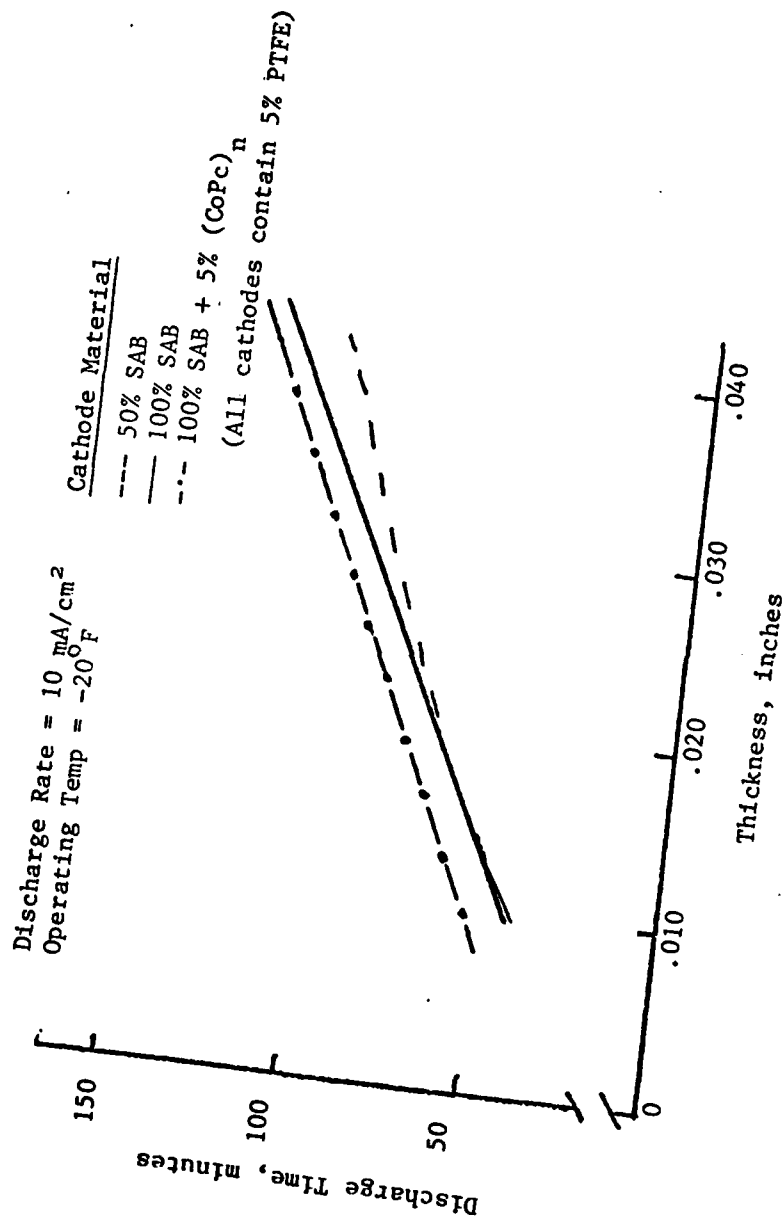


Figure 4. Effect of Carbon Substrates on the Li/SOCl<sub>2</sub> Cell Discharge Time in 1.5M LiAlCl<sub>4</sub>/SOCl<sub>2</sub> at -20°F.

The effect of cathode thicknesses on the overall discharge characteristics of  $\text{Li/SOCl}_2$  cells are shown in Figures 5 through 8 for various cathode compositions. With increased Teflon content in the cathode, the discharge time, in general, decreases, but cell voltage remains constant, within experimental error, for each cathode thickness. Catalyst doping (Figure 7 and 8) can be seen to improve both cell voltage and discharge time.

The discharge performance of  $\text{Li/SOCl}_2$  at  $-40^\circ\text{F}$  showed severe cell polarization with and without catalyst. The discharge characteristics were similar to the reported results<sup>(7)</sup>.

## B. PERFORMANCE OF OPTIMIZED CATHODES

### 1. Introduction

The systematic evaluation of baseline cathode performance since the start of this program has resulted in the optimization of cathode(s) for  $\text{Li/SOCl}_2$  cells. The optimized cathodes contain (by weight):

#### a) Baseline Cathode

- 95% - 100% compressed-grade Shawinigan acetylene black carbon substrate, (100% SAB).
- 5% - Teflon-6 binder

#### b) Catalyzed Cathode, $(\text{CoPc})_n$

- 5% - polymeric cobalt phthalocyanine
- 90% - 100% SAB
- 5% - Teflon-6

#### c) Catalyzed Cathode, FePc

- 95% - 100 SAB
- 5% - Teflon-6
- 2-5 mg of FePc/cc of electrolyte (both neutral and acidic electrolyte)



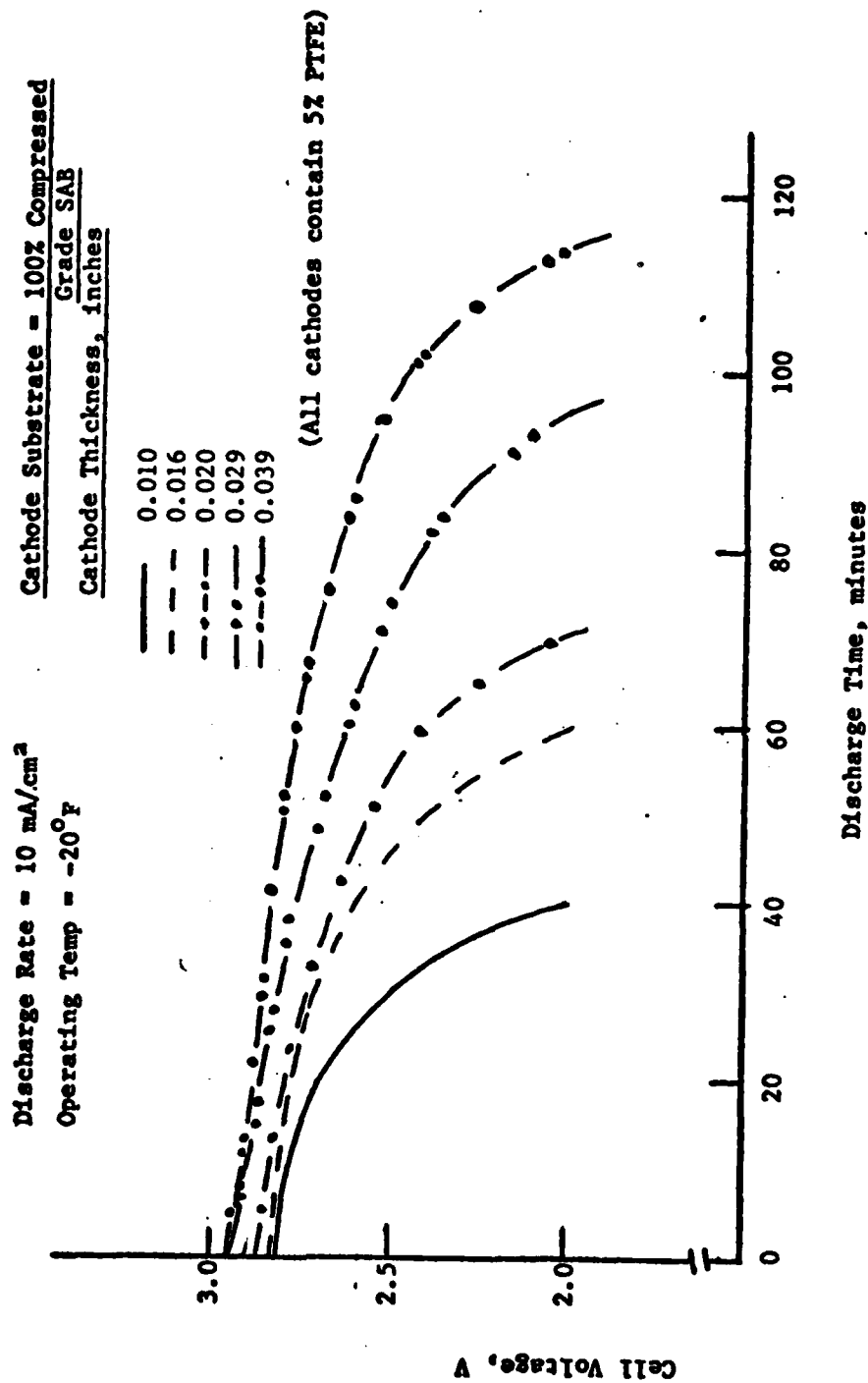


Figure 5. Effect of Cathode Thickness on Discharge Characteristics of 1.5M LiAlCl<sub>4</sub>/SOCl<sub>2</sub> Electrolyte

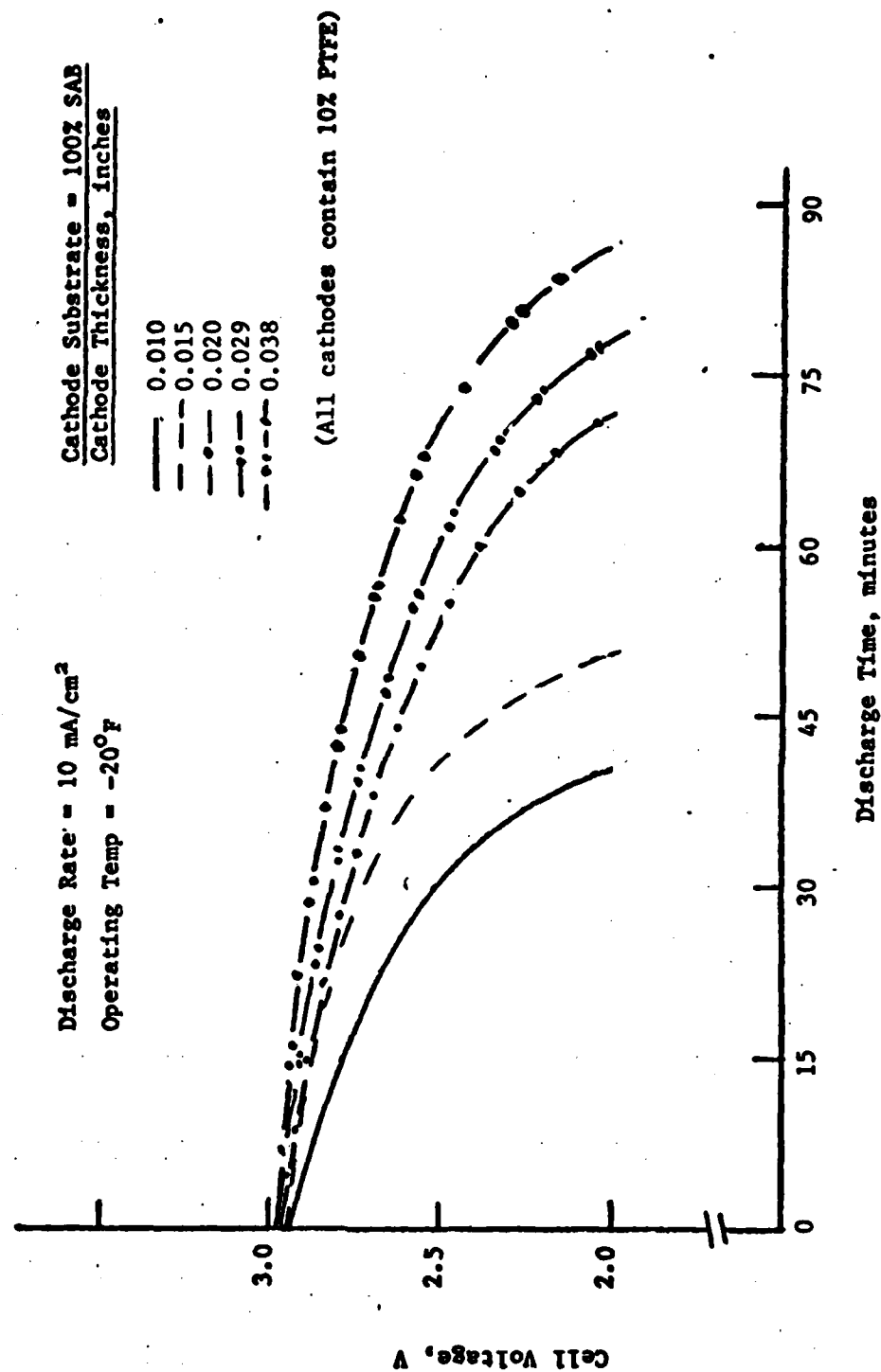


Figure 6. Effect of Cathode Thickness on Discharge Performance Characteristics of Li/SOCl<sub>2</sub> Cells with 1.5M LiAlCl<sub>4</sub>/SOCl<sub>2</sub> Electrolyte (10% PTFE).

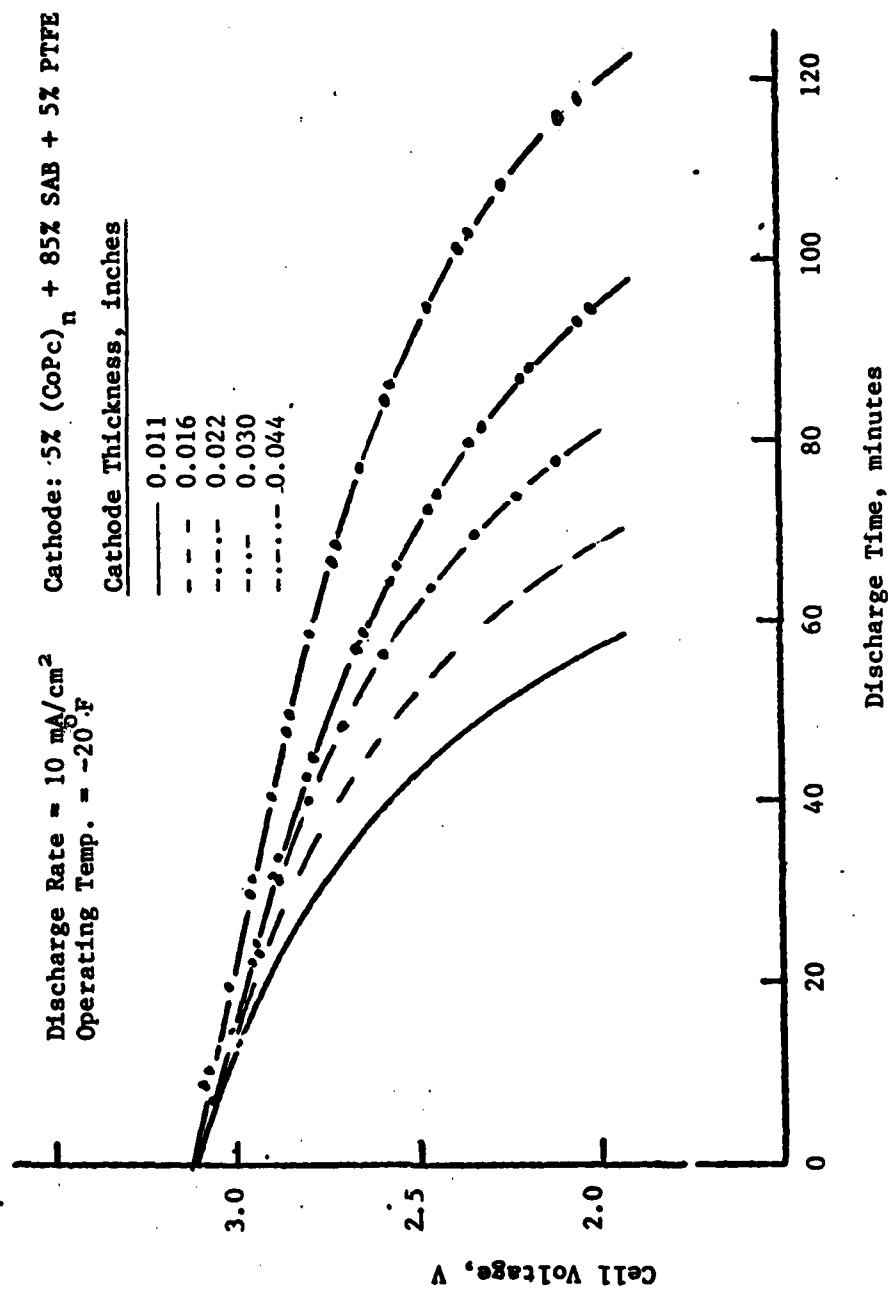


Figure 7. Effect of Cathode Thickness on Discharge Performance of Li/SOCl<sub>2</sub> with Catalyzed Cathode Containing 5% Teflon Binder in 1.5M LiAlCl<sub>4</sub>/SOCl<sub>2</sub>

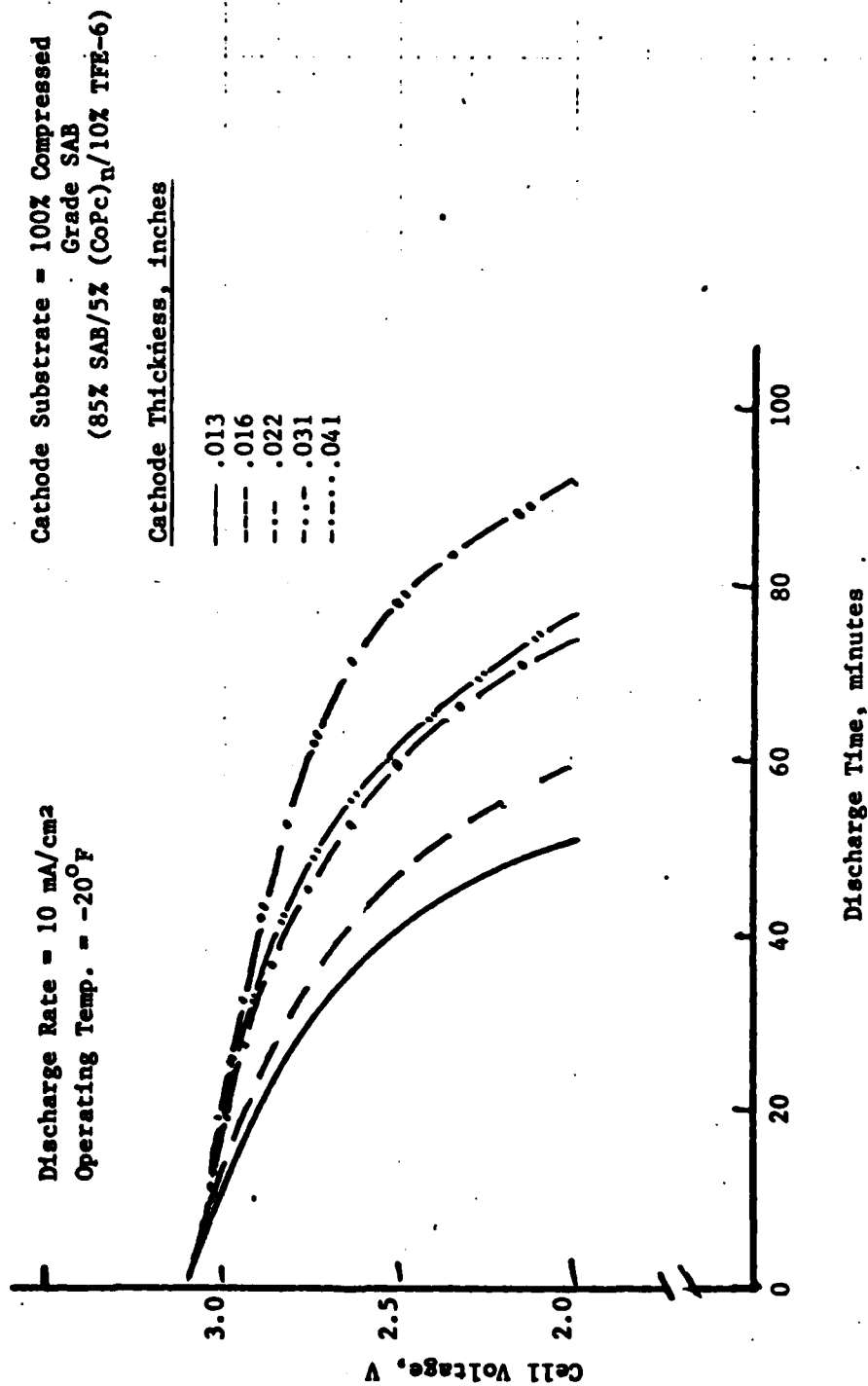


Figure 8. Effect of Cathode Thickness on Discharge Characteristics of Li/SOCl<sub>2</sub> Cells with Catalyzed Cathode Containing 10% Teflon Binder in 1.5M LiAlCl<sub>4</sub>/SOCl<sub>2</sub> Electrolyte.

## 2. Laboratory Cell Performance

The laboratory cell design and the description of cell components used in the evaluation of cathode polarization presented here have been described elsewhere<sup>(6)</sup>. Both half-cell measurements and cell discharge performance were made on the optimized cathodes at 75 and 32°F. Cathode thickness in all cases was 0.020 inch.

In Figure 9, the polarization characteristics of Li/SOCl<sub>2</sub> cells with 3 different cathodes are compared. With the catalyzed cathodes, cathode polarization decreased; the highest catalytic effect was achieved with FePc. The decrease in polarization is attributed to elementary processes taking place at the cathode (activation polarization). The effect of FePc doping further contributed to the higher cell limiting current. Therefore, it is assumed that the FePc catalyst not only enhanced the rate of electrochemical reduction of thionyl chloride but also modified the reaction mechanisms. This could potentially lead to a safer Li/SOCl<sub>2</sub> cell/battery.

The discharge performance of Li/SOCl<sub>2</sub> cells with and without catalyzed cathodes contributed to both high voltage and longer discharge time, as shown in Figures 10 through 13. FePc catalyzed cathodes showed the smallest cell voltage loss and the longest discharge life. The cell life increased by a factor of 2 over the uncatalyzed cathodes with FePc at 32 and 75°F.

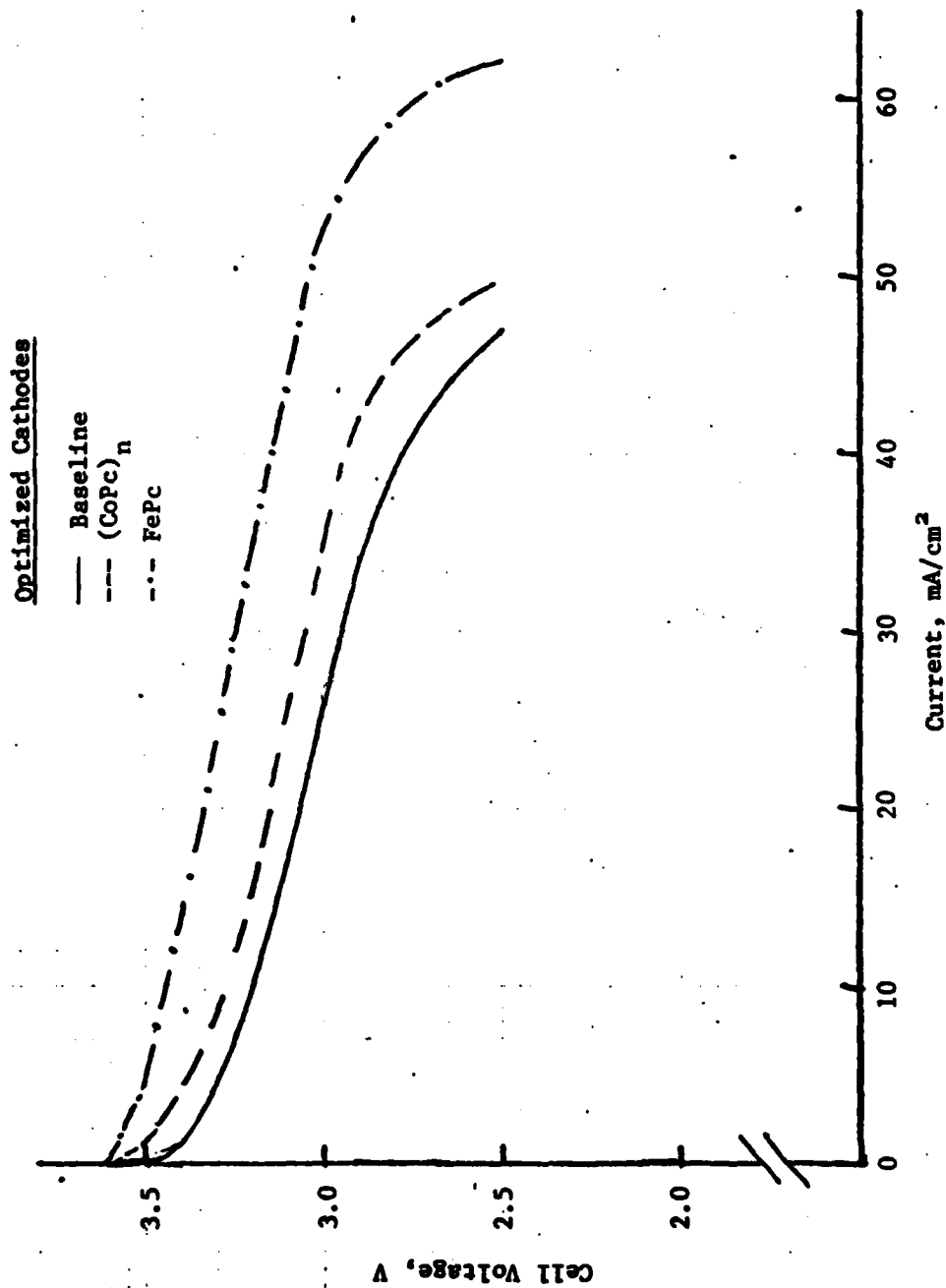


Figure 9. Polarization Characteristics of Li/SOCl<sub>2</sub> Cells at 75°F.

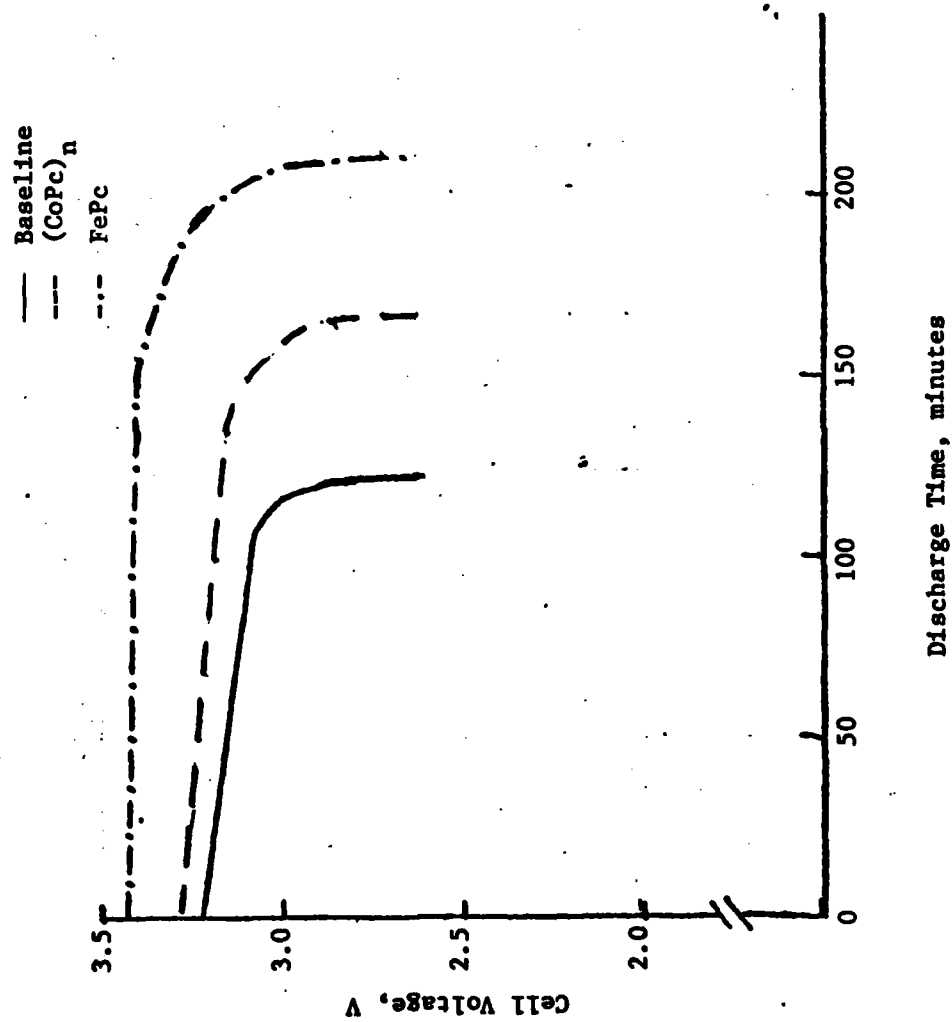


Figure 10. Discharge Characteristics of Li/SOCl<sub>2</sub> Cells at 10 mA/cm<sup>2</sup> and 75°F.

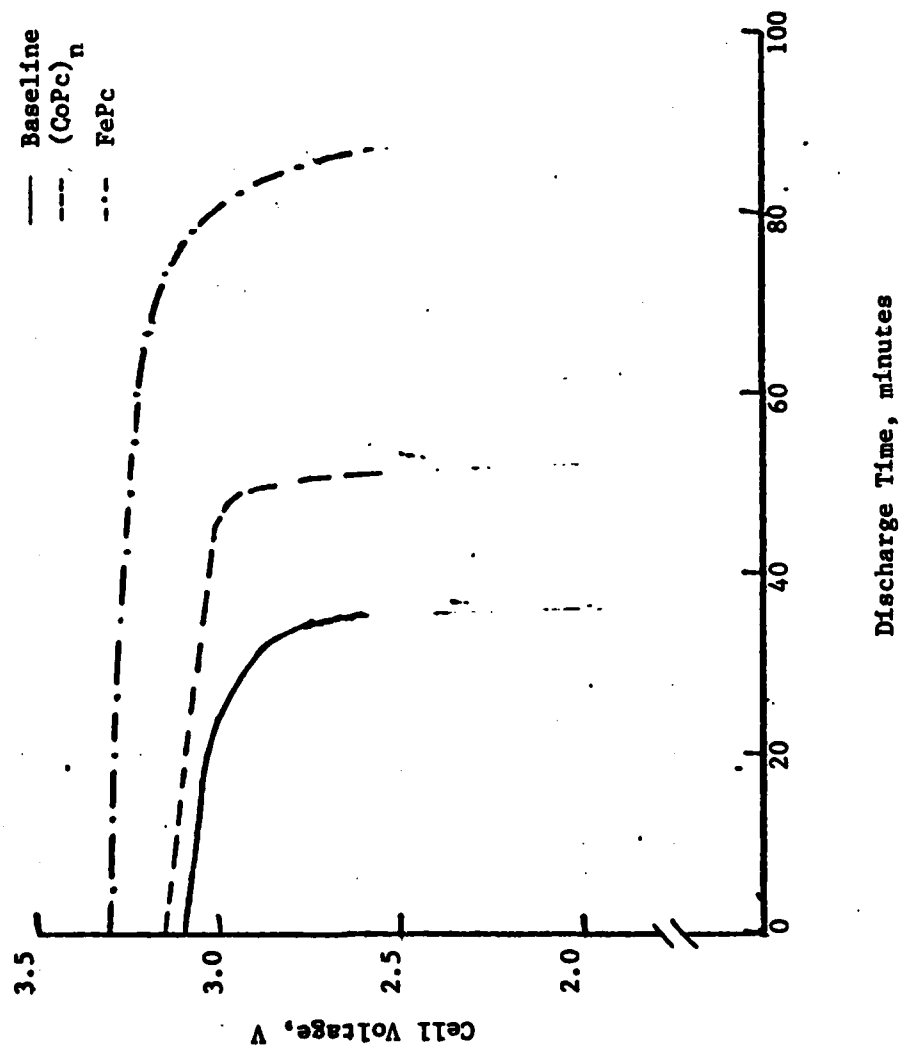


Figure 11. Discharge Characteristics of Li/SOCl<sub>2</sub> Cells at 20 mA/cm<sup>2</sup> and 75°F.



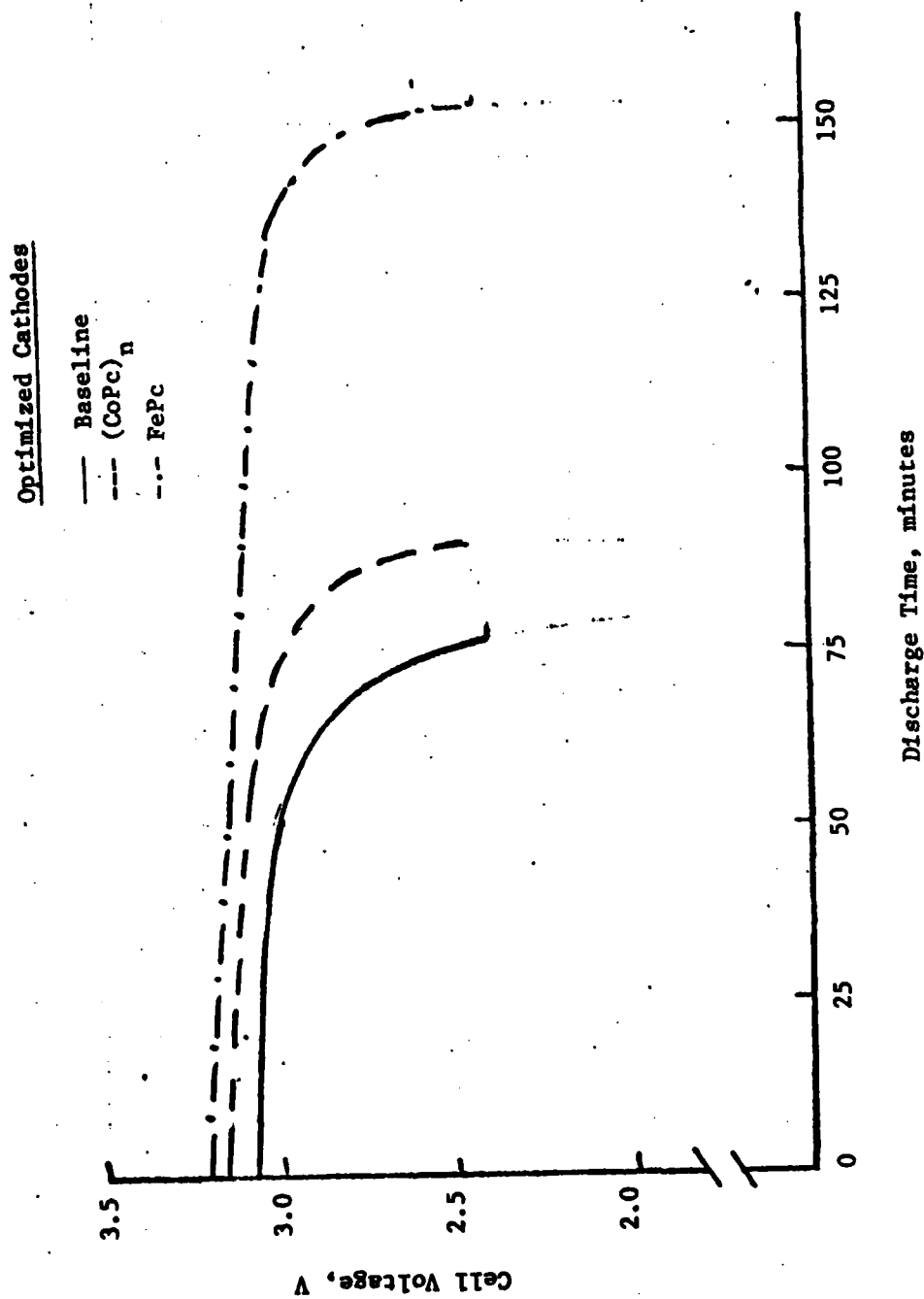


Figure 12. Discharge Characteristics of Li/SOCl<sub>2</sub> Cells at 10 mA/cm<sup>2</sup> and 32°F

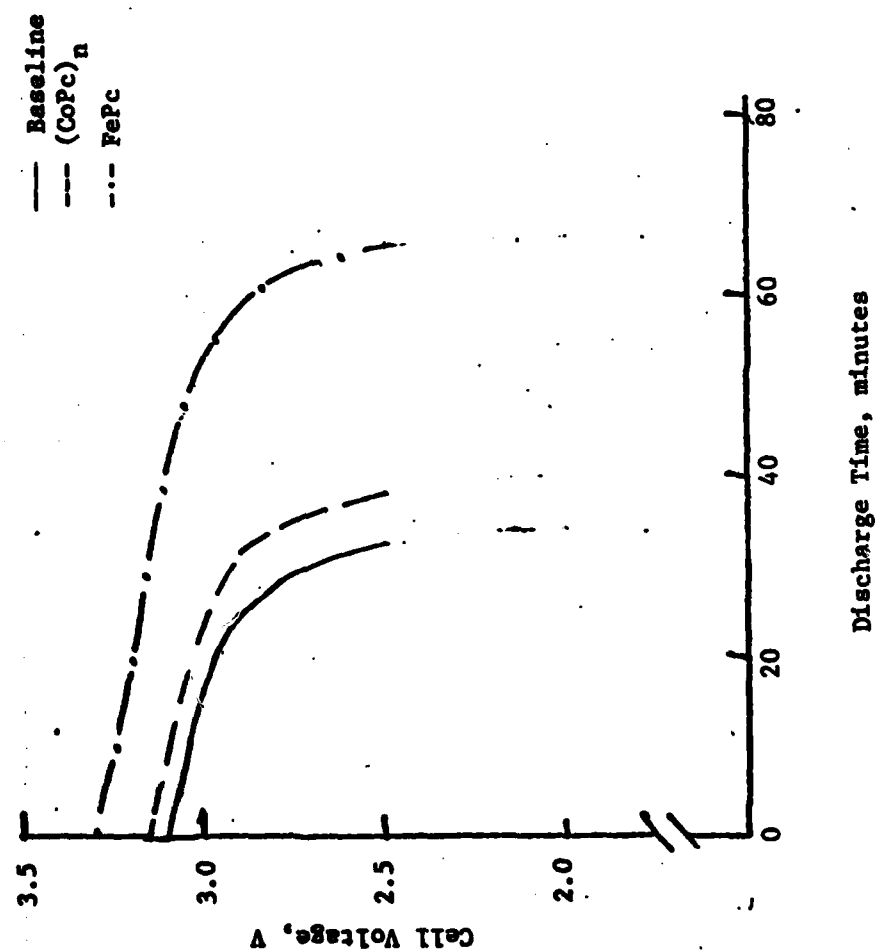


Figure 13. Discharge Characteristics of Li/SOCl<sub>2</sub> Cells at 20 mA/cm<sup>2</sup> and 32°F.

### III KINETIC AND MECHANISTIC STUDIES

The studies of electrode kinetics are important in understanding both the intermediate  $\text{Li/SOCl}_2$  reaction products and the reaction mechanism since these two important factors contribute to battery safety and performance. Cyclic voltammetric studies in 1.0M  $\text{LiAlCl}_4/\text{SOCl}_2$  solutions at various cathode surfaces indicate<sup>(6)</sup> that the system is diffusion controlled. However, it should be noted that the reaction products which are strongly adsorbed on the cathodes, and the diffusion limitations, might have contributed to the current peak heights in cyclic voltammograms. Therefore cyclic voltammetric studies were carried out at a rotating disc electrode.

Cyclic voltammograms were obtained at a glassy carbon electrode (  $0.458 \text{ cm}^2$  ). An ASR rotator, manufactured by Pine Instrument Company, was used to rotate the disc electrode. Cyclic voltammograms were generated using PAR electrochemistry system Model 170.

As a first order reaction mechanism, the experimental currents in a rotating disk study are related to the rotation rate  $\omega$  (in rpm) by the equation

$$\frac{1}{i} = \frac{1}{i_k} + \frac{1}{B\sqrt{\omega}} \quad (1)$$

where  $i_k$  is the kinetic current and B is a constant:

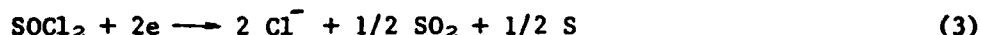
$$B = \frac{\sqrt{2\pi}}{\sqrt{60}} \quad n \cdot F \quad \nu^{1/2} \quad C_0 \left[ 0.621 \text{ s}^{-2/3} (1 + 0.298 \text{ s}^{-1/3} + 0.145 \text{ s}^{-2/3}) \right] \quad (2)$$

where  $\nu$  = kinematic viscosity  
 $F$  = The Faraday constant  
 $n$  = The number of electrons per mole of electroactive species  
 ( $\text{SOCl}_2$  in our case)  
 $C_0$  = The concentration of  $\text{SOCl}_2$  in moles/ $\text{cm}^3$   
 $S = \nu/D$ , where  $D$  = diffusion coefficient

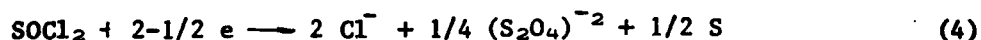
Figure 14 shows the plots of  $i_p^{-1}$  vs  $\omega^{-1/2}$  from the rotating disc data for  $\text{SOCl}_2$  reduction at glassy carbon electrode ( $0.458 \text{ cm}^2$ ) in  $1.5\text{M LiAlCl}_4/\text{SOCl}_2$  with and without FePc catalyst. At limiting currents, i.e., peak heights ( $i_p$ ), the currents usually correspond to pure diffusion control for the  $\text{SOCl}_2$  reduction. However, the plots indicate that the kinetic currents (intercepts) contribute to the limiting currents at  $100 \text{ mV/second}$  scan rate. Furthermore, in the presence of FePc catalyst, the kinetic current contribution to the limiting currents increases by 2.5 times (from  $25.24 \text{ mA/cm}^2$  to  $63.1 \text{ mA/cm}^2$ ). The  $i_k$  values decrease with decreasing scan rate in both cases. The  $i_p^{-1}$  vs  $\omega^{-1/2}$  plots from the rotating disc data obtained at different scan rates in FePc added to  $1.5\text{M LiAlCl}_4/\text{SOCl}_2$  electrolyte show (Figure 15) decreased kinetic currents with decreasing scan rate.

From the slopes of the straight lines in Figure 14, the B value can be calculated. For a similar reaction mechanisms, the slopes should be equal as the changes in the values of parameter in equation 2 are minimal with the addition of FePc catalyst to the electrolyte. However, in the presence of FePc catalyst, the B value increases from 0.467 to 0.633. This increase could be attributed to the modification in the overall reaction mechanism as follows:

At baseline cathode:



At FePc catalyzed cathode:



Plots of  $i_p^{-1}$  vs  $\omega^{-1/2}$  yield parallel straight lines at potentials anodic to the maximum (Figure 16), indicative of a first order process on  $\text{SOCl}_2$ . Deviation from parallel straight lines at more anodic potential could be due to changes in the reaction mechanisms. Further studies are needed to more fully understand the phenomenon.

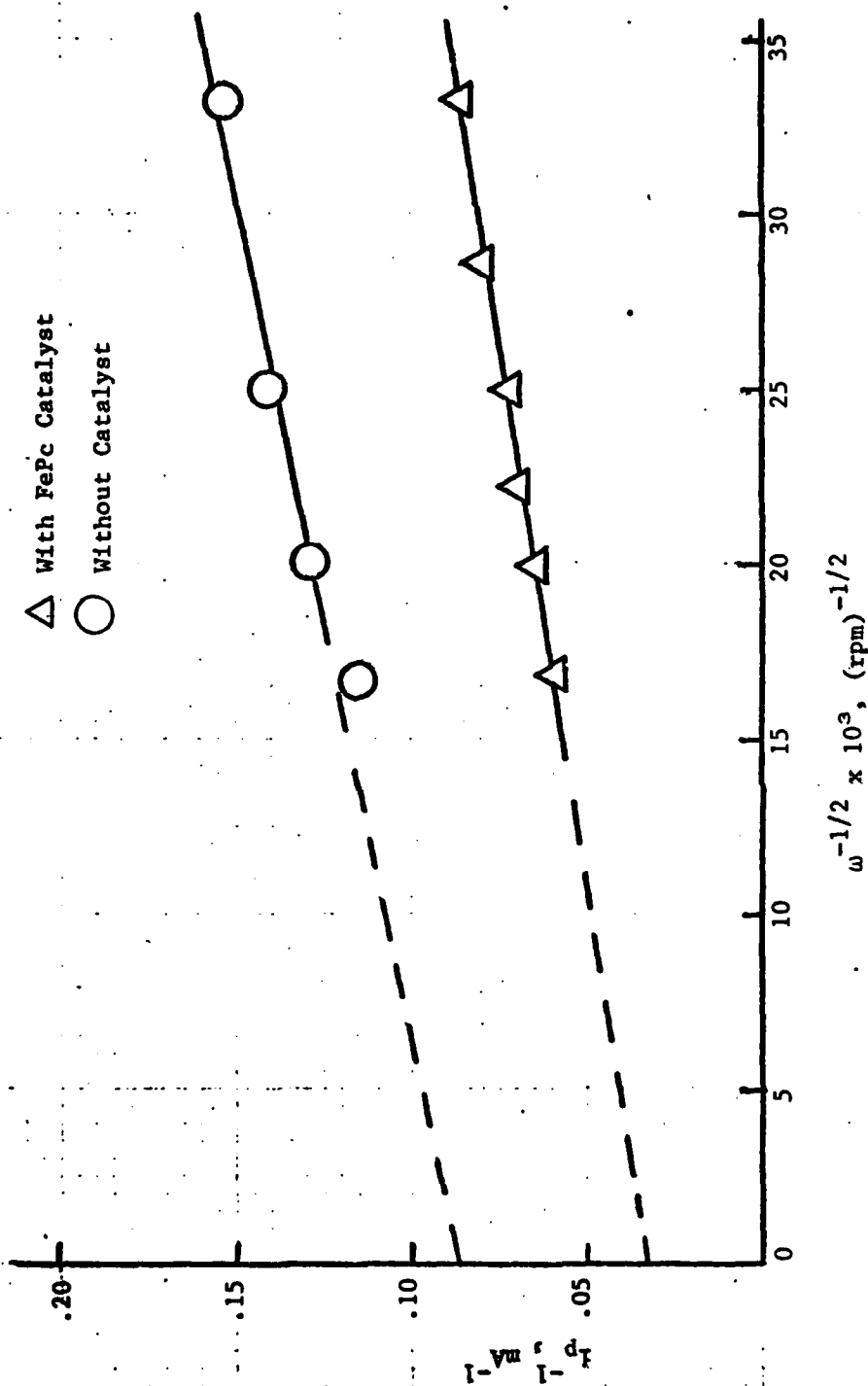


Figure 14. Plot of  $1/i_p$  VS  $1/\omega$  From the Rotating Disk Data for Glassy Carbon Electrode ( $0.458 \text{ cm}^2$ ) in  $1.5\text{M LiAlCl}_4/\text{SOCl}_2$  at Room Temperature, (Scan Rate  $100 \text{ mV/second}$ )

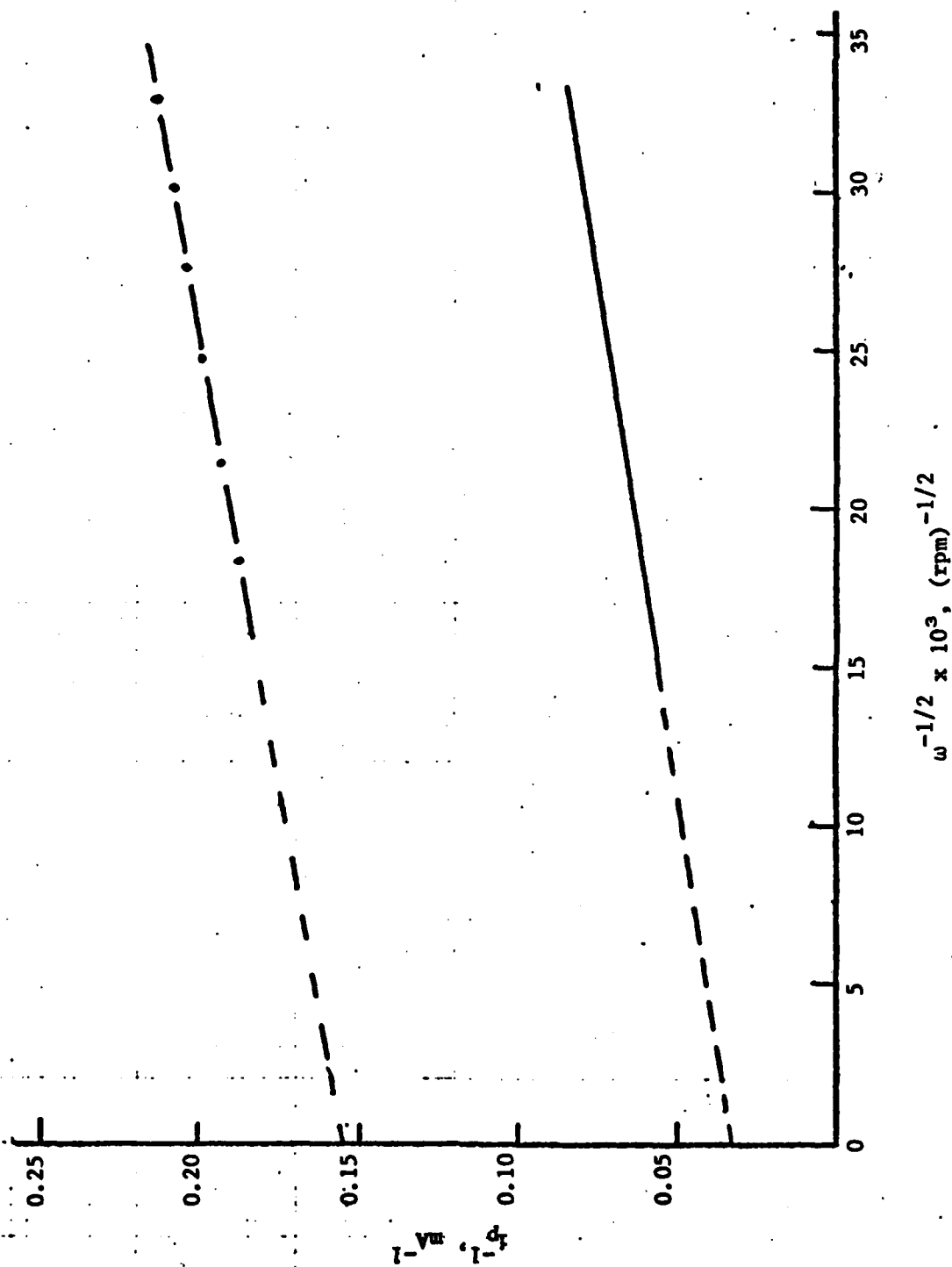


Figure 15. Plots of  $I_p^{-1}$  vs  $\omega^{-1/2}$  From the Rotating Disc Data for Glassy Carbon Electrode (0.458 cm<sup>2</sup>) in 1.5M LiAlCl<sub>4</sub>/SOCl<sub>2</sub> + FePc at Different Scan Rates (— 100 mV/seconds, --- 1 mV/seconds)

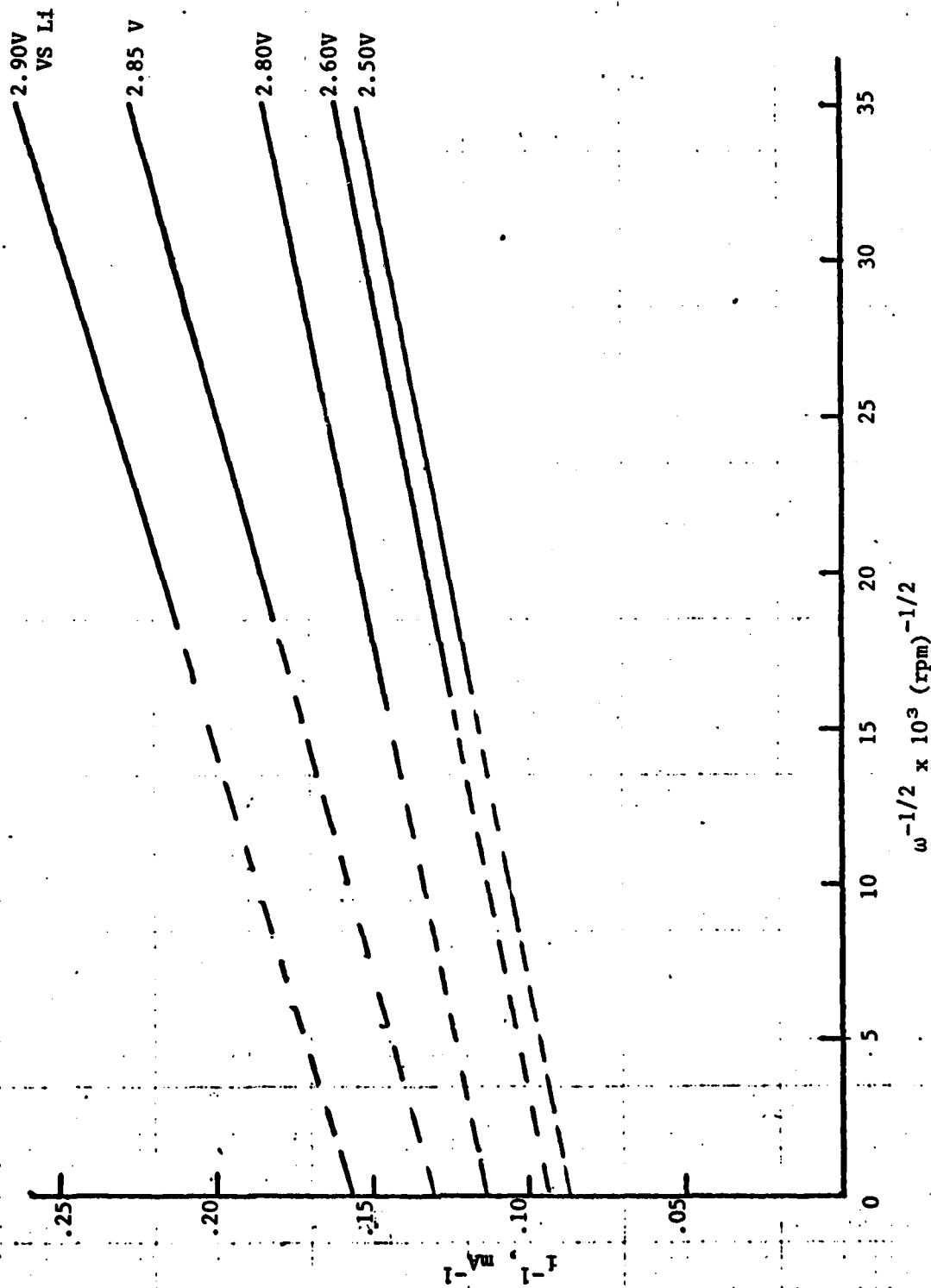


Figure 16. Plot of  $i^{-1}$  VS  $\omega^{-1/2}$  at Different Potentials From the Rotating Disc Data for Glassy Carbon Electrode (0.458 cm<sup>2</sup>) in 1.5M LiAlCl<sub>4</sub>/SOCl<sub>2</sub> at RT.

## IV AC IMPEDANCE MEASUREMENTS

### A. INTRODUCTION

Physical and chemical processes taking place at the electrode interface influence the overpotential of an electrode system. There are three types of processes which contribute to the total electrode overpotential; they are:

- a) activator overpotential
- b) concentration overpotential
- c) ohmic overpotential

All three types of overpotential contribute to cathode polarization in a Li/SOCl<sub>2</sub> system. The magnitude of each type depends on the operating current density, temperature, electrolyte conductivity and viscosity. In order to minimize the overall cathode potential, it is important to understand and evaluate each type.

Two non-steady state measurement techniques, galvanostatic single current pulse and AC impedance measurements are generally used to determine the type and magnitude of overpotentials. Recent successful AC impedance measurements studies<sup>(8,9)</sup> of lithium anodes prompted us to utilize this technique for porous electrode.

Alternating current impedance measurements are attractive to kinetic reaction studies, but the interpretation of experimental data obtained on a porous electrode can cause substantial complications, especially when adsorption and desorption processes are involved. However, recent advances in electronics have enabled the acquisition of a complete impedance spectrum within minutes by the use of the fast Fourier transform (FFT) algorithm, which allows Fourier analyses to be carried out readily upon complex input signals.

The theory of electrochemical impedance measurements of porous electrodes is very complex and will not be given here. Basically, a spectrum analyzer determines



impedance spectra by noise response impedance analysis; a white noise source generated by an analyzer is delivered to the cell and the current response is subjected to FFT analysis. The frequency dependent impedance and phase angle are displayed in the CRT and can be recorded easily.

## B. EXPERIMENTAL

AC impedance data were obtained at Sandia National Laboratories\* using a Hewlett Packard 3722A noise generator and a PAR Potentiostat 173. A Hewlett-Packard 9845T desk top computer was used to reduce the data. Impedance measurements at both steady state and dynamic conditions were made over the frequency range of 0.01 Hz to 1000 Hz.

The electrochemical cell consisted of a carbon electrode and a platinum counter electrode. Impedance measurements of the cathodes were made with and without iron phthalocyanine catalyst in 1.5M LiAlCl<sub>4</sub>/SOCl<sub>2</sub> electrolyte (3 mg FePc cc of electrolyte). Initial impedance experiments of baseline porous carbon electrodes with and without catalyst revealed that the electron transfer process was extremely slow at open circuit voltage and the impedance spectrum had a very large diameter. In order to minimize problems associated with high surface area porous electrodes, a stress annealed pyrolytic graphite electrode ( $A = 0.178 \text{ cm}^2$ ) was used.

## C. RESULTS

In Figures 17 and 18, the complex impedance of carbon electrodes with and without FePc catalyst respectively, in 1.5M LiAlCl<sub>4</sub>/SOCl<sub>2</sub> electrolyte are given. The diameter of the semicircle represents the Faradaic resistance if the capacitance value is small. For a diffusion controlled reaction, a straight line with a phase angle of 45° is usually obtained in the complex impedance. For a porous electrode the phase angle should be 22°.

The impedance of carbon electrodes in 1.5M LiAlCl<sub>4</sub>/SOCl<sub>2</sub> with and without FePc catalyst shows a semicircle with a large diameter. The diameter decreases with FePc catalyst. Still, very high resistance due to charge transfer process exists,

---

\* Experiments were carried out by Dr. Frank M. Delnick of Sandia National Laboratories

which is indicative of very slow reaction rates at open circuit voltage. The open circuit potentials vs platinum electrode were  $-0.322\text{V}$  and  $-0.511\text{V}$  for cathodes with and without FePc catalyst.

Impedance measurements were made on catalyzed cathodes under dynamic conditions. Figures 19 through 21 show the complex impedance at discharge rates of 34, 112 and  $675\text{ }\mu\text{A}/\text{cm}^2$ . The current rates remained constant at 34 and  $112\text{ }\mu\text{A}/\text{cm}^2$  throughout the experimented time (30 minutes at each experiment); however the discharge current,  $675\text{ }\mu\text{A}/\text{cm}^2$  decreased slowly with time ( $675\text{ }\mu\text{A}/\text{cm}^2$  to  $450\text{ }\mu\text{A}/\text{cm}^2$ ). At 34 and  $112\text{ }\mu\text{A}/\text{cm}^2$  discharge, the charge transfer resistance decreased but the reaction rates were still very slow. At  $675\text{ }\mu\text{A}/\text{cm}^2$ , the reaction is completely diffusion controlled as shown in Figure 21 by a straight line with a phase angle of  $42^\circ$ . Furthermore, when the impedance measurements were made at open circuit voltage after passing  $675\text{ }\mu\text{A}/\text{cm}^2$  current for nearly 30 minutes, as shown in Figure 22, the reaction is still diffusion controlled.

Additional experiments are needed to understand and establish various resistances (ionic, faradaic, etc.) which contribute to the cathode overpotential.

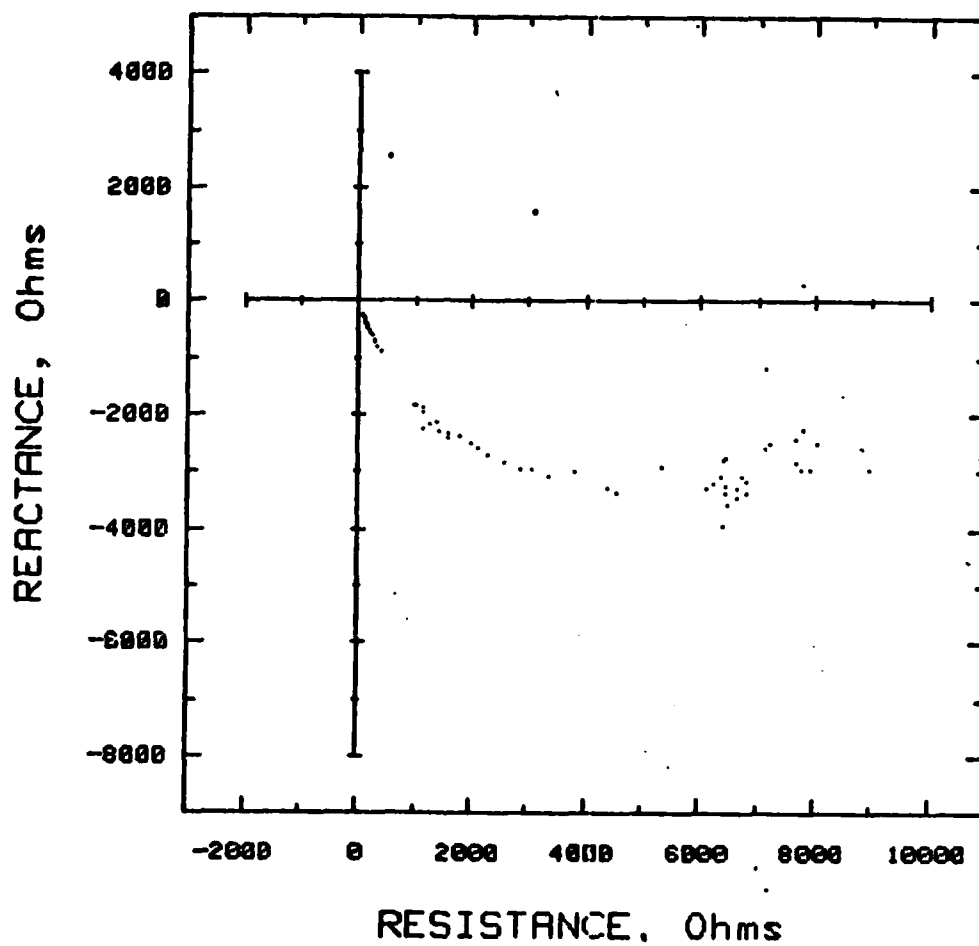


Figure 17. Impedance of Stress Annealed Pyrolytic Graphite Electrode ( $0.178 \text{ cm}^2$ ) in  $1.5\text{M LiAlCl}_4/\text{SOCl}_2$  Containing FePc Catalyst.

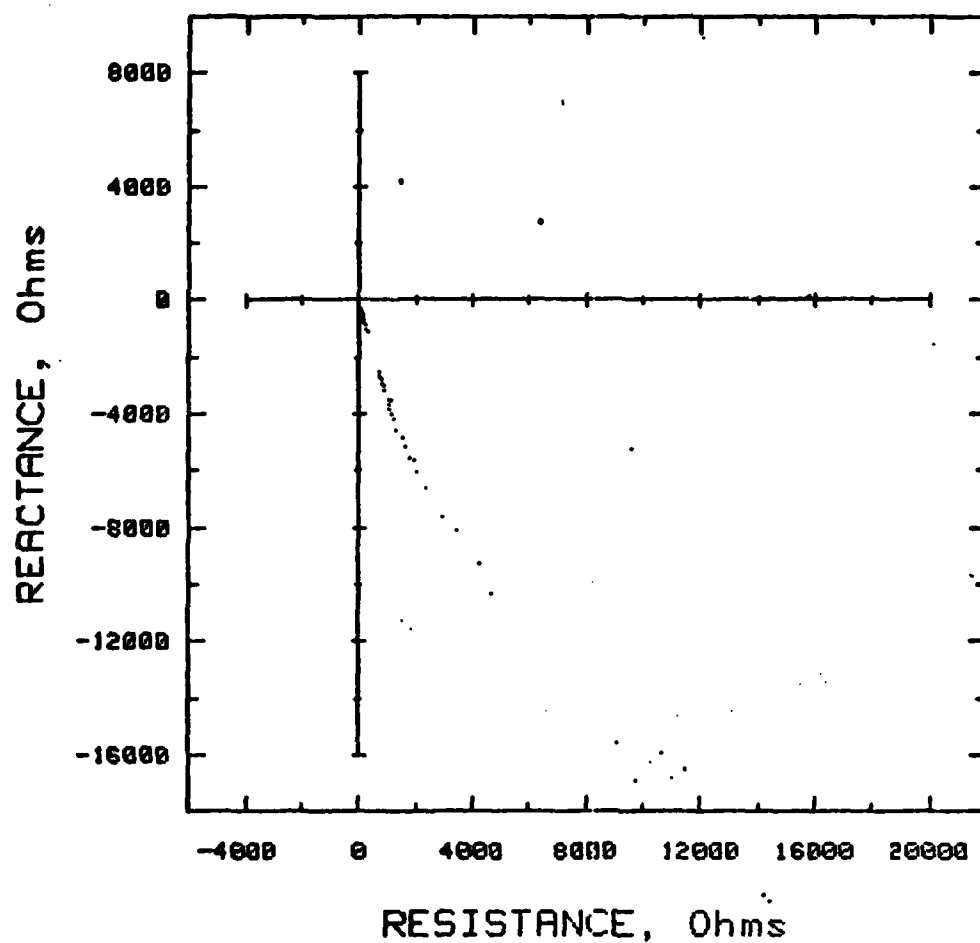


Figure 18. Impedance of Stress Annealed Pyrolytic Graphite Electrode ( $0.178 \text{ cm}^2$ ) in  $1.5\text{M LiAlCl}_4/\text{SOCl}_2$  Electrolyte at  $75^\circ\text{F}$ .

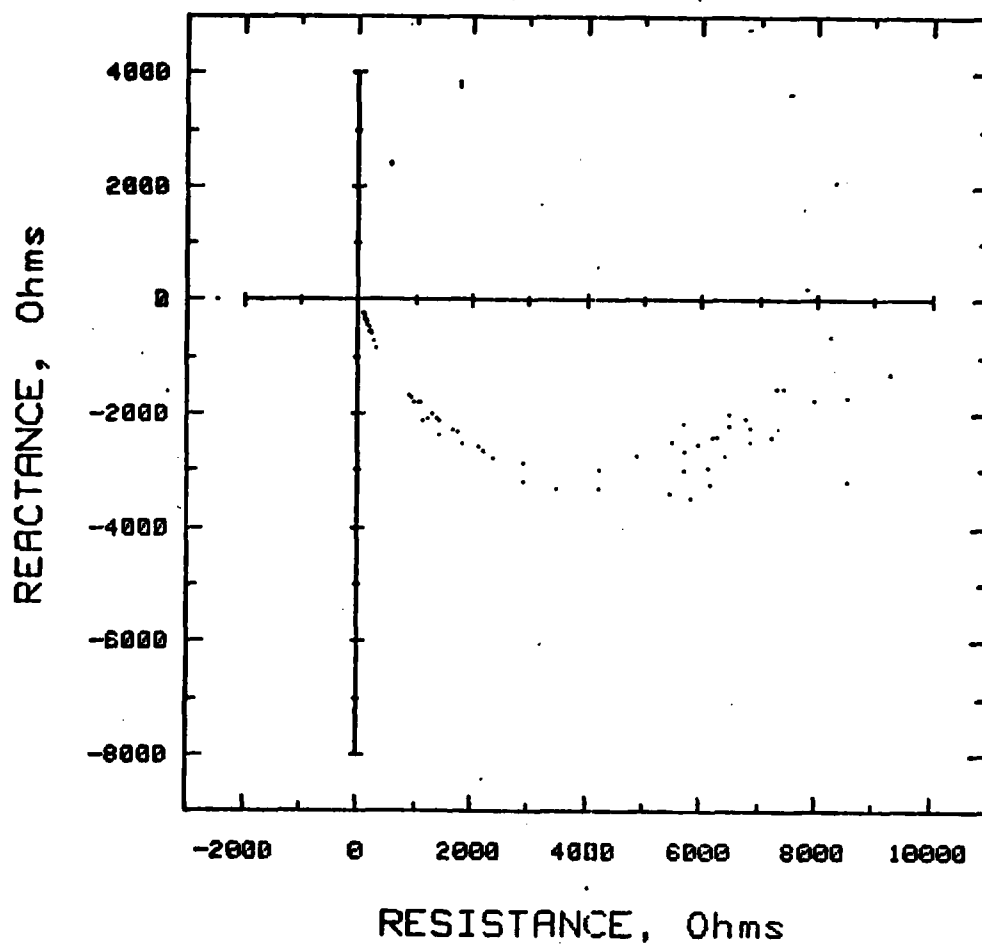


Figure 19. Impedance of Stress Annealed Pyrolytic Graphite Electrode (0.178 cm<sup>2</sup>) at a Discharge Rate of 34  $\mu$ A/cm<sup>2</sup> in 1.5M LiAlCl<sub>4</sub>/SOCl<sub>2</sub> + FePc.

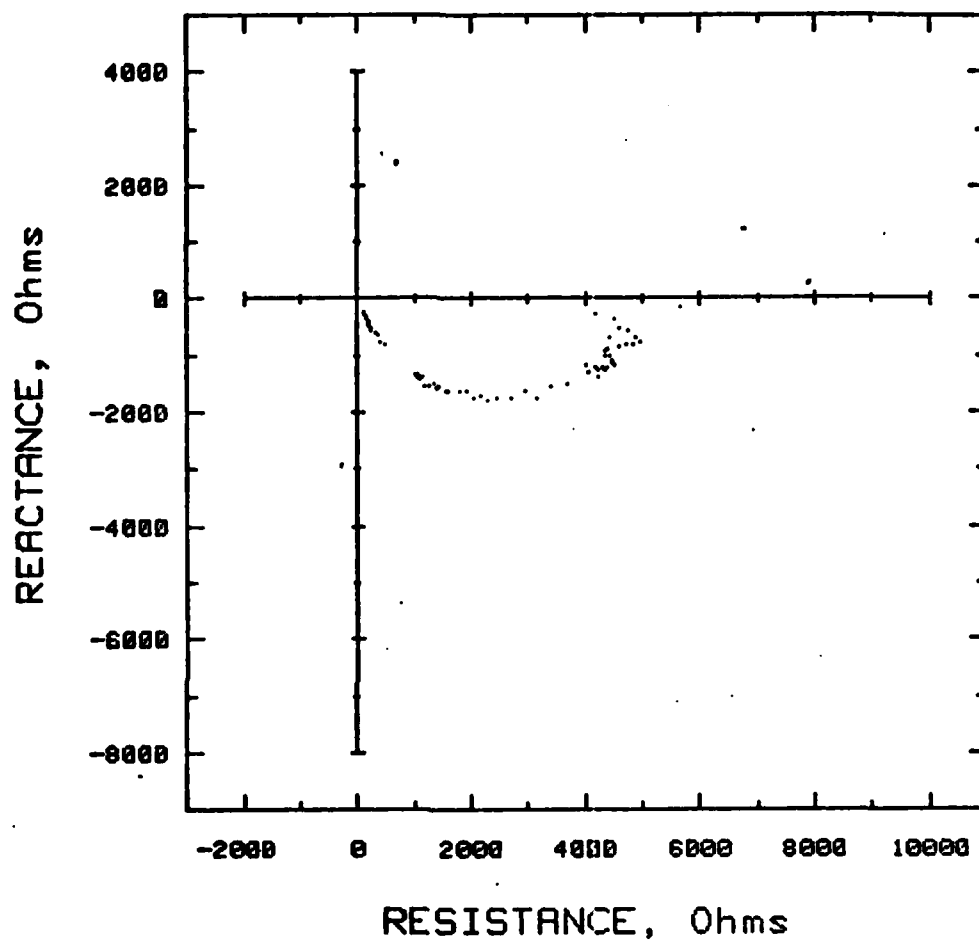


Figure 20. Impedance of Stress Annealed Pyrolytic Graphite Electrode ( $0.178 \text{ cm}^2$ ) at a Discharge Rate of  $112 \mu\text{A}/\text{cm}^2$  in  $1.5\text{M LiAlCl}_4/\text{SOCl}_2 + \text{FePc}$ .

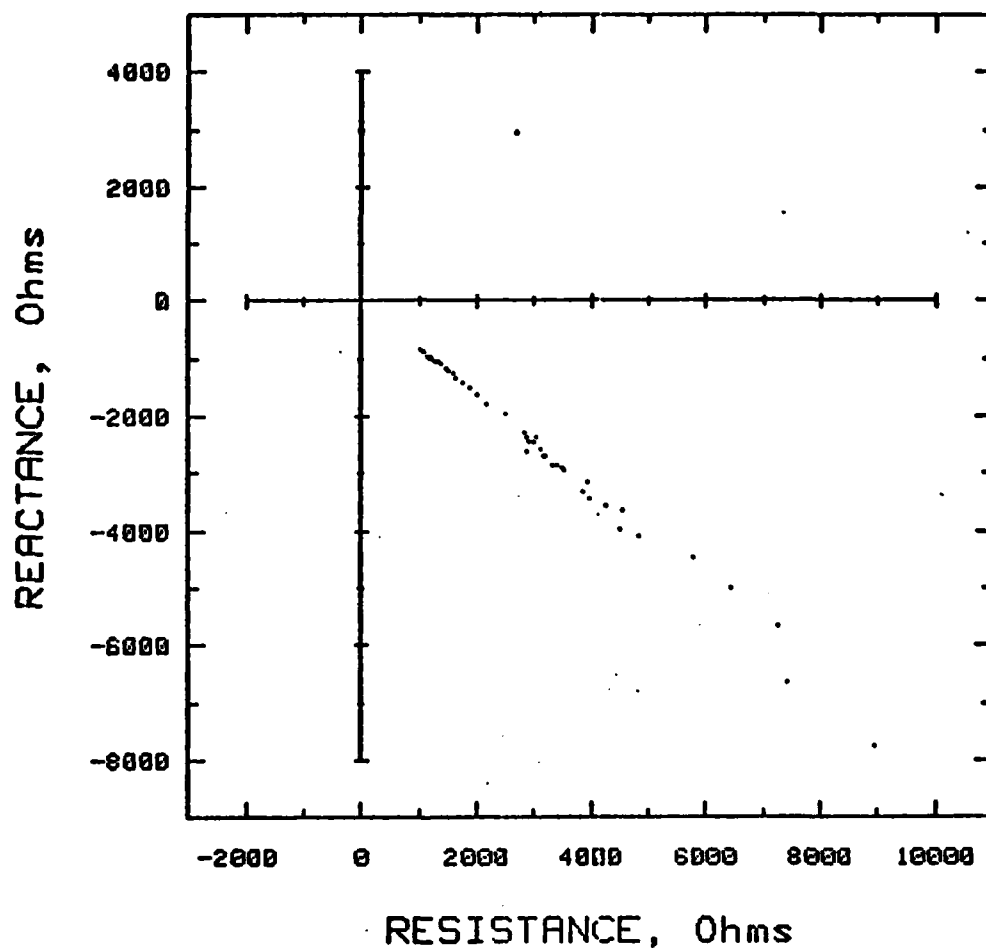


Figure 21. Impedance of Stress Annealed Pyrolytic Graphite Electrode ( $0.178 \text{ cm}^2$ ) at a Discharge Rate of  $675 \mu\text{A}/\text{cm}^2$  in  $1.5\text{M LiAlCl}_4/\text{SOCl}_2 + \text{FePc}$ .

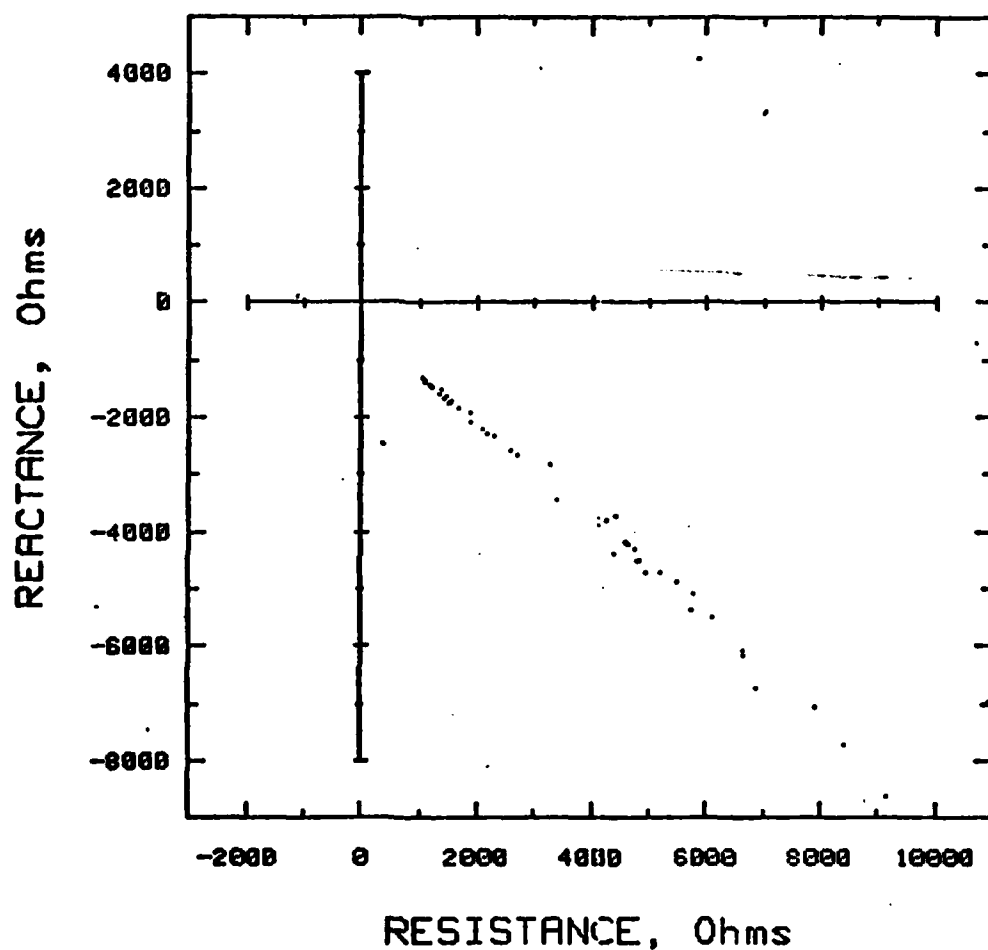


Figure 22. Impedance of Stress Annealed Pyrolytic Graphite Electrode ( $0.178 \text{ cm}^2$ ) at Open Circuit Voltage (After 30 minutes at  $675 \mu\text{A}/\text{cm}^2$  discharge) in  $1.5\text{M LiAlCl}_4/\text{SOCl}_2 + \text{FePc}$ .



## V. SUMMARY AND FUTURE WORK

During the third quarter, cathode optimization with respect to specified variables was completed. Performance evaluation of optimized cathodes at 32 and 75°F showed both catalyst B and C [FePc and (CoPc)<sub>n</sub>] minimized the electrode overpotential.

Plots of  $i_p^{-1}$  vs  $\omega^{-1/2}$  from rotating disc electrode studies produced parallel straight lines, indicative of a first order reaction mechanism. The slope of the straight line decreased with FePc catalyzed cathodes. This could indicate a change in reaction mechanism.

AC impedance measurements of a carbon electrode indicated extremely slow charge transfer and at high discharge rates, the rates were purely diffusion controlled.

During the last quarter of the program, we will carry out:

- Performance evaluation of optimized cathodes at 0 and -20°F.
- Continued rotating disc electrode studies at low temperatures.
- Writing of final report.

## REFERENCES

1. W. K. Behl, J. A. Christopoulos, S. Ramirez and S. Gilman, J. Electrochem. Soc. 120, 1619 (1973).
2. J. J. Auborn, K. W. French, S. I. Lieberman, V. K. Shah and A. Heller, J. Electrochem. Soc. 120, 1613 (1973).
3. G. E. Blomgren, V. Z. Leger, T. Kalnoki-Kis, M. L. Kronenberg and R. J. Brodd, in "Power Sources", J. Thomson, Editor, p. 583, Academic Press, (1979).
4. A. N. Dey, Thin Solid Films, 43, 131 (1977).
5. N. Doddapaneni, Extended Abstracts of the Electrochemical Society, Vol. 81-1, 218-219 (1981).
6. N. Doddapaneni, High Efficiency Lithium-Thionyl Chloride Cell, First Quarterly Report, DELET-TR-81-0381-1. Honeywell Power Sources Center, October 1981.
7. N. Doddapaneni, High Efficiency Lithium-Thionyl Chloride Cell, Second Quarterly Report, DELET-TR-81-0381-2, Honeywell Power Sources Center, January 1982.
8. J. Phillips, J. C. Hall and H. F. Gibbard, Extended Abstracts of Electrochem. Soc., Vol. 80-2, 165-167, (1980)
9. F. M. Delnick and C. D. Jaeger, Extended Abstracts of Electrochem. Soc. Vol. 81-2, 223-225 (1981).
10. V. G. Levich, "Physicochemical Hydrodynamics", Prentice Hall, Englewood Cliffs, NJ (1962).

# DISTRIBUTION LIST

Defense Technical Info Ctr ATTN: DTIC-TCA Cameron Station (Bldg 5) Alexandria, VA 22314	(12)	Commander US Army Electronics R&D Command Fort Monmouth, NJ 07703	
Cdr, Naval Surface Weapons Ctr White Oak Laboratory ATTN: Library, Code WX-21 Silver Spring, MD 20910	(1)	DELET-DD DELET-DT DELS-D-L (Library) DELS-D-L-S (Stinfo) DELET-PR (S. Gilman)	(1) (1) (1) (2) (20)
Commandant, Marine Corps HQ, US Marine Corps ATTN: Code LMC, INTS (In Turn) Washington, DC 20380	(1)	NASA Scientific & Tech, Info Facility Baltimore/Washington Intl Airt PO Box 8757, MD 21240	(1)
Rome Air Development Center ATTN: Documents Library (TSLD) Griffiss AFB, NY 13441	(1)	CMDR, MICOM ATTN: DRCPM-HDE Redstone Arsenal, AL 35809	(1)
AFGL/SULL S-29 HAFB, MA 01731	(1)	Foote Mineral Company Route 100 Exton, PA 19341 ATTN: Dr. H. Grady	(1)
HQDA (DAMA-ARZ-D/Dr. F.D.Verderame) Washington, DC 20310	(1)	Eagle-Picher Industries, Inc. Electronics Division P.O. Box 47 Joplin, Missouri 64801 ATTN: Mr. Robert L. Higgins	(1)
Cdr, Harry Diamond Laboratories ATTN: Library 2800 Powder Mill Road Adelphia, MD 20783	(1)	Yardney Electric Company 82 Mechanic Street Pawcatuck, CT 06379 ATTN: Technical Library	(1)
Director US Materiel Sys Anal Actv ATTN: DRXSY-T Aberdeen Prov Grnd, MD 21005	(1)	Duracell International, Inc. Northwest Industrial Park Burlington, MA 01803 ATTN: Dr. A.N. Dey	(1)
Cdr, USA Signals Warfare Lab ATTN: DELSW-OS Vint Hill Farms Station Warrenton, VA 22186	(1)	Exxon Research & Engineering Co. Corporate Research Laboratory Linden, NJ 07036 ATTN: Dr. R. Hamlen	(1)
Commander USA Mobility Eqp Res & Dev Cmd ATTN: DRDME-R Fort Belvoir, VA 22060	(1)	Argonne National Laboratories 9700 South Cass Argonne, IL 60439 ATTN: Dr. E.C. Gay	(1)
Cdr, Harry Diamond Labs ATTN: DELHD-CO,TD (In Turn) 2800 Powder Mill Road Adelphia, MD 20783	(1)		

General Motors Corp. Research Laboratories General Motors Technical Center 12 Mile and Mounds Roads Warren, MI 48090 ATTN: Dr. J.L. Hartman (1)	GTE Laboratories, Inc. 520 Winter Street Waltham, MA 02154 ATTN: Dr. Ronald McDonald (1)
Union Carbide Corporation Parma Research Center P.O. Box 6116 Cleveland, OH 44101 (1)	Electrochimica 2485 Charleston Road Mountain View, CA 94040 ATTN: Dr. Eisenberg (1)
Duracell International, Inc. S. Broadway Tarrytown, NY 10591 ATTN: J. Dalfonso (1)	Energy Storage & Conversion Dept. TRW Systems One Space Park Redondo Beach, CA 90278 ATTN: Dr. H.P. Silverman (1)
North American Rockwell Corp. Atomics International Division Box 309 Canoga Park, CA 91304 ATTN: Dr. L. Heredy (1)	Sanders Associates, Inc. 24 Simon Street Mail Stop NSI-2208 Nashua, NH 03060 ATTN: J. Marshall (1)
General Electric Research & Development Center P.O. Box 8 Schenectady, NY 12301 ATTN: Dr. Stefan Mitoff (1)	Power Conversion, Inc. 70 MacQuesten Pkwy Mount Vernon, NY 10550 ATTN: Stuart Chodosh (1)
University of California Department of Science & Research Santa Barbara, CA 93100 ATTN: Dr. J. Kennedy (1)	Portfolio Manager Hooker Chemicals & Plastics Corp. M.P.O. Box 8 Niagara Falls, NY 14302 (1)
Gulton Industries, Inc. Metuchen, NJ 08840 ATTN: Mr. S. Charlip (1)	G207 S.R.I. Menlo Park, CA 94025 ATTN: Dr. Leonard Nanis (1)
INCO Research and Development Center Sterling Forest Suffern, NY 10901 ATTN: Nehemiah Margalit (1)	Bell Laboratories 600 Mountain Avenue Murray Hill, NJ 07974 ATTN: Dr. J.J. Auborn, Rm 1A-317 (1)
Director Propulsion and Power Division Mail Code EP5 NASA-Johnson Space Center Houston, Texas 77058 ATTN: Mr. B. J. Bragg (1)	Jet Propulsion Laboratory 4800 Oak Grove Drive Pasadena, CA 91103 ATTN: Mr. Harvey Frank Mail Stop 198-220 (1)
	Naval Surface Weapons Center White Oak Laboratory, Code R-33 (M/S A026) Silver Spring, MD 20910 ATTN: Dr. D. Ernst (1)
	Energy Conversion Branch Code 3642 Naval Underwater Systems Center Newport Laboratory Newport, RI 02840 ATTN: Mr. J. R. Moden (1)

NASA Lewis Research Center  
Mail Stop 6-1  
21000 Brookpark Road  
Cleveland, OH 44135  
ATTN: Dr. Stuart Fordyce

(1)

EIC, Inc.  
Newton, MA 02158  
ATTN: S.B. Brummer

(1)

Altus Corp.  
440 Page Mill Road  
Palo Alto, CA 94306  
ATTN: Douglas Glader

(1)

MS 488  
NASA Langley Research Center  
Hampton, VA 23665  
ATTN: J. Bene

(1)

Research and Development Division  
The Gates Rubber Co.  
999 S. Broadway  
Denver, CO 80217  
ATTN: Mr. Eddie T. Seo

(1)

Mail Stop 8C-62  
Boeing Aerospace Company  
P.O. Box 3999  
Seattle, WA 98124  
ATTN: Mr. Sidney Gross

(1)

Honeywell Technology Center  
10701 Lyndale Avenue, South  
Bloomington, MN 55420  
ATTN: Dr. H.V. Venkatesetty

(1)

Jet Propulsion Laboratory  
M.S. 198-220  
4800 Oak Grove Drive  
Pasadena, CA 91103  
ATTN: Mr. Aiji Uchiyama

(1)

Naval Surface Weapons Center  
White Oak Laboratory, Code R-33  
Silver Spring, MD 20910  
ATTN: Dr. Frank Bis

(1)

Dr. Jerry J. Smith  
ONR Chemical Program  
Arlington, VA 22217

(1)

Saft Corporation of Aermica  
711-A Industrial Blvd.  
P.O. Box 1284  
Valdosta, GA 31601  
ATTN: Mr. Lou Adams

(1)

Gould Laboratories-Energy Research  
40 Gould Center  
Rolling Meadows, IL 60008  
ATTN: Dr. J. Hall

(1)

Electrochem Industries (E-I) Inc.  
9990 Wehrle Drive  
Clarence, NY 14031  
ATTN: Dr. C. Liang

(1)

GTE Laboratories Incorporated  
40 Sylvan Road  
Waltham, MA 02254  
ATTN: Dr. C. Schlaiker

(1)

Harvey N. Seiger Associates  
8 Beacon Hill Drive  
Waterford, CT 06385  
ATTN: Harvey N. Seiger, Ph.D.

(1)

DATE  
ILME  
—8